8-2015

Influence of low shear and cyclic strain on hyperglycemic rat aortic smooth muscle cells: An In Vitro dynamic disease model

Varun Chawla
Clemson University, vchawla@clemson.edu

INFLUENCE OF LOW SHEAR AND CYCLIC STRAIN ON HYPERGLYCEMIC RAT AORTIC SMOOTH MUSCLE CELLS: AN *IN VITRO* DYNAMIC DISEASE MODEL

A Thesis
Presented to
the Graduate School of
Clemson University

In Partial Fulfillment
of the Requirements for the Degree
Master of Science
Bioengineering

---

by
Varun Chawla
August 2015

Accepted by:
Dr. Martine LaBerge, Committee co-Chair
Dr. Agneta Simionescu Committee co-Chair
Dr. Dan Simionescu

Abstract

Vascular complications are the leading cause of morbidity and mortality amongst diabetic patients which represent a major proportion of patients undergoing coronary artery revascularization. Major advances in drug eluting stent technologies have reduced the overall rates of restenosis in general however diabetic patients still remain at a high risk thus requiring target lesion revascularization more commonly as compared to non-diabetic cohort. Phenotypic modulation demonstrated by smooth muscle cells is essential for normal wound healing response however is also contributive to initiation and development of various vascular complications including neointimal hyperplasia which ultimately leads to the lumen re-narrowing or restenosis. Hyperglycemia is the hallmark of diabetes with clinical evidence of poor glycemic control correlated with exaggerated neointimal hyperplasia. Although the contribution of phenotypic modulation to the development of restenosis has been well explored nevertheless, our understanding of this characteristic response in diabetic patients remains less understood. In the current study, the effects of acute and chronic hyperglycemia on vascular smooth muscle cell phenotypic modulation under mechanically loaded conditions were evaluated and current results suggests an exaggerated response in acute and chronic conditions. The long term goal of this project is to design an in vitro dynamic disease model which would compare cellular response to combined hemodynamic disturbances and metabolic abnormalities thus elucidating novel drug and targets aimed at reducing neointimal hyperplasia in diabetic patients.

Acknowledgements

I would like to express my sincerest thanks to the committee co-chair Dr. Martine LaBerge for providing me the opportunity to work on this research project. I am grateful to her for inculcating professionalism and passion for work in me. Dr. LaBerge has been a great source of motivation and support throughout this project. I would also like to extend my deepest thanks to the committee co-chair Dr. Agneta Simionescu for all the guidance and support. Her points of view helped me to figure out the big picture of this project. I am thankful to Dr. Dan Simionescu and Dr. Eugene Langan III for their valuable advice and critique to the project. My special thanks to the members of our lab especially Astha Khanna for all the support. I would also like to thank Dr. Bruce Gao and Godley-Snell animal facility for their donation of rats to this project. Finally, I am grateful to my family members for all their support.

Table of Contents

Page

List of Figures and Tables

Chapter 1: Introduction

1.1 Review of Literature

1.1.1 *Blood Vessel Anatomy:*

Blood is carried out through the body via blood vessels. Arteries carry blood away from the heart and branch into smaller vessels downstream. Arterioles, the smallest arteries, branch into tiny capillaries which are responsible for exchange of nutrients and wastes. These are connected to venules, which carry blood to veins and eventually return the blood to the heart [2]. A blood vessel comprises of three distinctive layers or tunics known as Intima, Media, and Adventitia.

Tunica Intima: It is the innermost layer of a blood vessel and is in direct contact with blood. Intima is composed of specialized squamous epithelial cell layer called the endothelium. The endothelium is embedded on a basal lamina or basement membrane which binds the endothelium to the underlying connective tissue. Primary role of the basement membrane is to provide mechanical strength while maintaining flexibility. In addition, the permeable nature of the basement membrane also permits materials to pass through it. In larger blood vessels, intimal layer also consists of an internal elastic membrane. In large arteries, a thick layer of elastic fiber also exists at the boundary with tunica media called the internal elastic lamina (IEL). In addition to providing structure while allowing the vessel to stretch, its permeable nature permits the transport of nutrient between the tunics [2].

Tunica Media: Generally the thickest layer in arteries, media consists of concentric layers of smooth muscle cells supported by a connective tissue network consisting primarily of elastic and collagenous fibers. Contraction and relaxation of circumferentially arranged muscular cells maintains the vascular tone of a blood vessel. During vasoconstriction, smooth muscle cells contract thus making the lumen narrower and increasing the blood pressure. Vasodilation leads to an increase in blood flow due to relaxation of smooth muscle cells which causes the lumen to widen. In large arteries, external elastic lamina (EEL) separates the media from the outermost layer of the blood vessel. [2].

Tunica Adventitia: The outermost layer which comprises of a sheath of connective tissue made up primarily of collagenous fibers and fibroblasts. It is the thickest layer in veins. In addition to providing a rigid mechanical support, adventitia connects the blood vessel to the surrounding connective tissue [2].

Depending on the distance from the heart, elastic fiber content in the intima and smooth muscle content in the media varies. Blood vessels closer to the heart, which are typically larger than 10 mm in diameter, are called elastic or conducting arteries. These are typically rich in elastic fibers, which enables them to expand and recoil with each cardiac cycle. The elastic recoil helps in maintaining the pressure gradient to drive the blood flow while offering a lower resistance to flow. Moving away from the heart, elastic fiber content in the intima of the arteries decreases while the amount of smooth muscle in the media increases. Such arteries range from 0.1 – 10 mm in diameter and branch into arterioles. These are known as Muscular or distributing arteries with a thicker media playing an important role in vasoconstriction [2].

1.1.2 *Blood Vessel Forces:* With each cardiac cycle, blood is transported to the aorta for distribution to the peripheral arteries under pulsatile pressure. Hence, the arteries are subjected to circumferential and longitudinal stresses. Blood pressure exerts a force perpendicular to the vessel wall which leads to a circumferential stretching of the wall and the respective stress is termed as circumferential stress. In contrast, force exerted by the flow, induced from the pressure gradient, leads to a stress and strain parallel to the surface of endothelial cells known as shear stress. [3]. Typical mean arterial values of shear stress range from 6 to 40 dyne/cm^2 but can vary from 0 to well over 100 dyne/cm^2 in the vasculature [4-6] whereas circumferential stress in a healthy human aorta ranges from 1 to 2 x 10^6 dynes/cm^2 depending upon the anatomical location [3]. Disturbances in these forces has been shown to affect local cellular homeostasis. Atherosclerosis, in humans, has been shown to be strongly correlated to sites where low time-averaged shear stress, shear stress reversal and spatial & temporal gradients in shear stress exist. Similarly, implants such as stents and

grafts also induce changes in the local mechanical forces and thus may also affect cellular function [4]. For evaluating the cellular response to altered shear stress, two common *In Vitro* systems have been used. Firstly, a parallel plate flow chamber in which cells are typically grown on a glass slide sandwiched between parallel polycarbonate plates. A small gap between the plates permits the circulation of the cell culture medium [4]. For Newtonian fluids flowing through a rectangular channel, wall shear stress is defined by:

$$T_W = \frac{6\mu Q}{bh^2}$$

where Q = volumetric flow rate, b = width of channel, h = height of channel, μ = viscosity.

The second system involves a cone and plate system in which a fixed angle cone rotates with an angular velocity and for small angles, shear rate (and therefore shear stress) is essentially constant throughout the flow field [4]. Tension in a blood vessel is commonly represented using Laplace's law given by:

$$T = Pr$$

where T = Tension in the vessel wall (dynes/cm), P = Blood pressure (dynes/cm^2) and r is the radius of the blood vessel. Wall (hoop stress, dynes/cm^2), which is the normal stress in the circumferential direction, is given by:

$$\sigma_\theta = T/t$$

where T = Tension in the vessel wall and t = wall thickness [7, 8].

Elastic properties of vessel wall are represented by apparent wall stiffness (or vascular compliance) and elastic modulus inherent to the wall. Vascular wall stiffness is expressed by the pressure-strain elastic modulus:

$$E_P = \Delta P_i / (\Delta D_0 / D_0)$$

where D_0 is the external diameter at pressure P_i and ΔD_0 is the change in external diameter due to change in pressure ΔP_i, at P_i. Vascular compliance is basically the inverse of wall stiffness for the respective area and volume components [9].

1.1.3 *Mechanotransduction:* It has been well established from various studies that cells recognize shear stress as a stimulus and thus initiate different signal transduction cascades in response to stress. Endothelial cells (EC), in particular, represent a well explored example. ECs have been shown to change their shape from polygonal, in static cultures, to elongated upon exposure to flow [10, 11]. In addition, ECs also increase production of vasodilators including nitric oxide (NO) [12-14] and prostacyclin [15] while decreasing the release of vasoconstrictor molecules like endothelin [16] and angiotensin-converting enzyme [17], when subjected to shear stress. Shear stress also increases the anti-thrombotic & fibrinolytic activity of ECs by upregulating the production of thrombomodulin [18] and plasminogen activators [19, 20].

Cells recognize mechanical forces as a stimulus through different membrane molecules and cellular micro-domains, which are commonly known as Mechanosensors. Typically, these include Ion channels, growth factor receptors, G-proteins, Caveolae, adhesion proteins, cytoskeleton, glycocalyx and primary cilia [19]. Ion channels of Ca^{2+}, K^+, Cl^-, Na^+ are activated by mechanical forces which leads to exchange of ions from extracellular space resulting in a change of membrane potential and intracellular ion concentration. G-protein coupled receptor activation increases the activity of adenylate cyclase (AC) and phospholipase C (PLC) which subsequently cause an increase in the secondary messengers like cyclic adenosine monophosphate (cAMP), Ca^{2+}, Inositol trisphospate (IP_3), and diaglycerol (DAG). cAMP further activates cAMP-dependent protein kinase A (PKA) which leads to phosphorylation of a variety of proteins. Cytosolic Ca^{2+} binds to calmodulin and activates the calmodulin-dependent kinase. IP_3 binds to its receptor on the endoplasmic reticulum and initiates a release of Ca^{2+} ions form intracellular stores. DAG leads to the activation of protein kinase C (PKC). Tyrosine kinase receptor-activation leads to increase in IP_3 and phosphorylation of small G proteins, such as Ras which causes activation of mitogen-activated

protein kinase (MAPK). In addition, cell adhesion proteins such as Integrins phosphorylate focal adhesion kinase (FAK) located in the focal contact with the extracellular matrix (ECM) [19].

Similarly, in response to cyclic stretch, mechanosensors are also responsible for signal transduction in vascular smooth muscle cells (VSMCs). Interaction of VSMC integrins with the ECM plays an important role in initiation of mechanotransduction by stretch. Response of VSMCs to stretch is dependent upon specific ECM molecules thus suggesting the involvement of integrins [21]. Activation of receptor tyrosine kinases such as platelet-derived growth factor receptor alpha (PDGFα) has been shown to be stretch-magnitude dependent in VSMCs. This PDGFα activation was shown to be independent of autocrine or paracrine release of PDGF by VSMCs [22]. In addition, stretch can also lead to phosphorylation of epidermal growth factor receptor (EGFR) and its recruitment of adaptor proteins Shc and Grb2 which, in turn, lead to extracellular-regulated kinase ½ (ERK ½) activation [23]. Finally, stretch can also activate non-selective ion channels which allow the exchange of K^+, Ca^{2+}, Na^+ ions [21].

1.1.4 *Atherosclerosis:* Atherosclerosis is a chronic disease of the arterial wall and is the leading cause of death and loss of productive life years worldwide. Atherosclerotic lesions are asymmetrical focal thickenings of the innermost layer of the artery. They consist of cells, connective-tissue elements, lipids and debris. Blood-borne inflammatory and immune cells constitute an important part of the atherosclerotic lesion with the remainder of the cells being endothelial and vascular smooth muscle cells. The atheroma is preceded by a fatty streak, an accumulation of lipid-laden cells beneath the endothelium. Most of the cells in the fatty streak are macrophages, together with some T-cells [24].

Role of Endothelial Cells: The primary role of the endothelium is to maintain vascular hemostasis by a variety of regulatory substances including Nitric Oxide, prostaglandins, angiotensin and Endothelin-1. Upon activation, endothelial cells can upregulate adhesion molecules such as Intercellular adhesion molecule-1 (ICAM-1), VCAM-1, P-selectin to promote the attachment and

rolling of circulating leukocytes and platelets. In addition to vasodilation and vasoconstriction, an intact endothelium inhibits platelet activation and inflammation by reducing the upregulation of these platelets and leukocyte adhesion molecules [25].

Role of Inflammatory cells: Monocyte activation and subsequent transformation to macrophages is a key step involved in the development and progression of atherosclerosis. At an early stage, monocytes transmigrate into the intima and differentiate to macrophages. Formation of foam cells, a hallmark of atherosclerosis, results from uptake of oxidized LDL (oxLDL) molecules by macrophages. In addition, macrophages also secrete cytokines and growth factors (including MCP-1 & MCF-7) which encourage recruitment of more leukocytes from the circulation [26]. Activation of macrophages subsequently leads to the release of smooth muscle growth regulatory molecules thus initiating migration and proliferation of smooth muscle cells.

Role of Vascular Smooth muscle cells: Growth factors and cytokines released by platelets and inflammatory cells lead to phenotypic modulation of underlying smooth muscle cells leading to their migration and proliferation into the intima. This response continues uninhibited and is accompanied by accumulation of new extracellular matrix. Increased secretion of local MMPs is also contributive to the migration of VSMCs. In addition, VSMC are also believed to confer plaque stability as of fibrous caps with reduced muscle cells is more susceptible to rupture [27].

Role of Hemodynamics:

Various studies have demonstrated that in spite of numerous contributing factors to development of atherosclerosis, local hemodynamics play an extremely important role as atherosclerosis is a geometrically focal disease preferentially affecting the outer edges of vessel bifurcations. Focal propensity of atherosclerosis is believed to be mediated due to atherogenic endothelial phenotype as a consequence of low wall shear stress acting on these cells [28].

Studies with animal models and in humans have shown that focal activation of the endothelium, in large and medium-sized arteries, may initiate the development of atherosclerosis. Endothelial cells normally resist attachment of the white blood cells streaming past them, but upon activation from the stimulus, they express adhesion molecules that capture leukocytes on their surfaces [29]. Simultaneous changes in the permeability of the endothelium and the underlying matrix promote the entry and retention of cholesterol-containing low-density lipoprotein (LDL) particles in the artery wall [30]. Modification of LDL, through oxidation or enzymatic attack in the intima, leads to the release of phospholipids that can activate endothelial cells to express several types of leukocyte adhesion molecules, including vascular-cell adhesion molecule 1 (VCAM-1), which is typically upregulated in response to hypercholesterolemia and preferentially promotes monocyte and lymphocyte adhesion since they carry the counter-receptors for VCAM-1 [31]. Cheomattractants, produced in the underlying intima, mediate the direct migration of the bound leukocytes into the sub-endothelial space [24]. Monocytes entering the intima are stimulated by macrophage-colony stimulating factor (MCSF) to differentiate into macrophages with upregulation of scavenger-receptors and toll-like receptors on their surface, which consequentially leads to engulfment of oxidized lipid molecules by macrophages to become lipid-laden foam cells [29]. Accumulation of lipid-laden foam cells beneath the endothelium leads to the formation of fatty-streaks, which is the first sign of atherosclerosis.

Lesion progression: Macrophages engulfing the modified lipoproteins produce cytokines and growth factors, which in turn cause further recruitment of the macrophages and vascular smooth muscle cells from the underlying medial layer. In particular, interleukin-1 (IL-1) and tumor necrosis factor-alpha (TNF-α) stimulate the local production of PDGF and fibroblast-growth factor (FGF), which cause the migration and proliferation of VSMCs from the media to the intima. An important step in the migration and proliferation of SMCs is believed to be the secretion of the matrix metalloproteinases (MMPs), especially MMP-9, which are responsible for the degradation of the

internal elastic lamina in cerebral arteries and abdominal aorta [32]. Lipoprotein lipase released by the endothelium can cause proliferation of SMCs. This process involves a series of steps that include protein kinase-C activation and binding of lipoprotein lipase to the VSCM proteoglycans [33-35] and results in switching off the gene expressing the contractile proteins and switching on the genes for synthetic activity. Synthetic VSMCs synthesize and produce extracellular matrix [36] and help in further progression towards a stable atherosclerotic plaque. Acting in tandem, all of these factors lead to the formation of a fibro-fatty lesion [37]. A thick fibrous cap confers stability on the plaque by reducing the circumferential tensile stress and prevents contact between the lipid-rich necrotic core and the blood. However, a thin cap typically has collagen-poor structure with few SMCs but abundant macrophages [29] and also experience tensile stress and are predisposed to rupture [37]. Plaque macrophages and SMCs can also die in advancing lesion, some by apoptosis and cause release of extracellular lipids and cell debris which further can accumulate in the central region of a plaque and is often denoted as the lipid or necrotic core [29].

Clinical complication: Plaques generally cause clinical manifestations by producing flow-limiting stenosis that lead to tissue ischemia or more commonly they can embolize and lodge in distal arteries. Inflammatory cells may hasten the plaque disruption by elaborating collagenolytic enzymes that can degrade collagen and by generating mediators that provoke the death of SMCs, which is the source of arterial collagen [38]. Production of MMPs has been identified as the most significant factor in this regard. In a fibrous cap, stromelysins activate other members of the family, degrade a broad spectrum of peptides that include proteoglycans, type IV collagen, fibronectin and laminin and can also destroy the matrix proteins of the cap and thus increase the likelihood of rupture [38].

Clinical Intervention for treating atherosclerosis:

For atherosclerotic lesions requiring surgical intervention, three main procedures are commonly used- Balloon angioplasty, Stenting, Coronary artery bypass graft (CABG).

Coronary Artery Bypass Graft: For multi-vessel lesions, diabetes mellitus, severe ventricular dysfunction patients, coronary arterial or vein graft is a suitable surgical procedure. In addition, polymeric grafts made from Dacron polyester or polytetrafluoroethylene (PTFE) are also available.

Angioplasty: This procedures involves compression of the atherosclerotic plaque in order to restore flow. During this procedure, a catheter is inserted usually into the femoral artery with a deflated balloon on a catheter tip. The most commonly used materials for manufacturing balloons are polyethylene (PE) or polyethylene terephthalate (PET). Balloons are available in different diameters and length depending upon the lesion site. At the lesion site, a balloon is inflated with saline typically to pressures of about 5-15 atm. Mechanistically, balloon expands until the deployment forces equals vessel wall circumferential force. The net result is reopening of the blood vessel [39].

Stenting: A stent is a mesh-like scaffold that prevents the negative recoil of blood vessel after angioplasty. The expansion of a stent to its yield strength ensures that the stent does not collapse. Commonly used materials for stents include stainless steel, cobalt-chromium, platinum-titanium alloys, nickel-titanium, tantalum alloys. In addition to providing a scaffold for prevention of negative recoil, stents have also been designed to slowly release drugs in order to control neointimal hyperplasia. First-generation drug-eluting stents include Paclitaxel eluting stents (Taxus, PES) and Sirolimus eluting stents (Cypher, SES). Paclitaxel cause microtubular arrest through polymerization of alpha and beta-tubulin in the cytoskeleton. Paclitaxel causes the cell cycle arrest at the G2/M phase of mitosis. In contrast, Sirolimus inhibits the mammalian target of rapamycin (mTOR) and thus causes cell cycle arrest at the G1 phase. A common clinical problem with first-generation DES was the late-stent thrombosis and inflammation in response to the thick polymer coating [40]. Second generation DES include zotarolimus-leuting stent (Endeavor, ZES) and everolimu-eluting stents (Xience V, EES) and also bio-degradable polymer coated biolimus-ES [41].

1.1.5 ***Restenosis:*** Percutaneous coronary intervention (PCI) procedures such as balloon angioplasty and stenting are commonly used to treat clinical symptoms of atherosclerosis. A major drawback of (PCI) is restenosis of the treated vessel, resulting in renewed symptoms and the need

for repeat intervention. Binary angiographic restenosis is defined as the re-narrowing of the vessel lumen to >50% occlusion, usually within 3-6 months after PCI. Clinical restenosis is characterized by recurrent angina pectoris requiring target vessel revascularization (TVR) [42]. Restenosis is a common problem after balloon angioplasty with rates of up to 50-60% [43, 44].However, with the introduction of bare metal stents these rates have diminished to 20-30% and with drug eluting stents it has dropped down to an overall 5-10% incidence [45]. Despite the major advances in interventional cardiology, restenosis remains a consistent clinical problem owing to the in-stent restenosis and late catch-up phenomenon with drug-eluting stents and an economic burden due to the large number of procedures performed world-wide annually.

Pathophysiology: It has been suggested that restenosis is a maladaptive response of the blood vessel to trauma induced during angioplasty with the sequence of events– thrombosis, inflammation, cellular proliferation and extracellular matrix production that, in concert, contribute to post-procedural lumen loss over approximately 6 month [46]. Lumen loss after balloon angioplasty can be separated into 3 distinct stages: Early loss associated with elastic recoil, late loss due to negative remodeling, and neointimal hyperplasia. Elastic recoil occurs immediately following angioplasty with reports of 34% loss in lumen diameter within 15 minutes of balloon inflation and may account for up to 50% of loss in the acute lumen gain after angioplasty [46-49].

Fracture of the atherosclerotic plaque exposes the thrombogenic contents to the bloodstream thus triggering platelet adhesion, activation and thrombosis. This is further complicated by the denudation of the endothelium which leads to the loss of antithrombogenic factors like Nitric oxide (NO), prostacyclin and tissue plasminogen activator. Platelets, upon activation, release mitogens including thromboxane A_2, serotonin and platelet-derived growth factor (PDGF) which leads to phenotypic modulation of medial smooth muscle cells resulting in their migration to the intima, proliferation and synthesis of extracellular matrix [46]. Negative remodeling may also contribute to the development of restenosis as replacement of hyaluronic acid with collagen in the extracellular matrix is believed to result in scar contraction [50, 51].

With stents, elastic recoil is virtually eliminated and neointimal hyperplasia is the main mechanism responsible for lumen narrowing after stent implant and thus in the development of in-stent restenosis [52]. Cellular mechanisms leading to development of in-stent restenosis (ISR) have been described to be a part both the early and late phase of the complication. The early phase, immediately after the intervention, is associated with relocation of plaque, reorganization of thrombus and an acute inflammatory response. Thrombus formation seems to be a consequence of the endothelial disruption [53] thus leading to deposition of fibrin and platelets at the site of injury which invoke an inflammatory response. Consequently, an increased leukocyte trafficking is evident at the stent location with subsequent migration into the media [54]. Increased production of adhesion molecules, cytokines, chemoattractants and growth factors by corroborating platelets, monocyte/macrophages and SMCs in turn results in an increased recruitment of inflammatory cells. With the onset of the late phase, phenotypic modulation of VSMCs results in their migration into the intima and subsequent proliferation. Extensive extracellular matrix (ECM) production by dedifferentiated cells is responsible for the increasing volume of the intimal tissue with the bulk of the neointimal tissue comprising primarily of proteoglycans and collagen with late lesions consisting of only about 11% cellularity [55, 56].

The advent of Drug-eluting stents (DES) has reduced the overall rates of restenosis as compared to Bare-metal stents (BMS) alone. However, with the increasing use of DES, especially in complex lesions such as lesions in left main artery, bifurcations, small vessel vein grafts, chronic total occlusions and diabetic patients, ISR rates of up to 10% have been reported [57, 58]. The time frame to restenosis after DES may be longer as compared to BMS due to the application of anti-proliferative drugs with repots of up to 12 months [59]. Various factors, similar to BMS, have been implicated in the development of ISR with DES including diabetes, lesion length, vessel diameter, implantation factors. In addition to these, factors such as resistance to antiproliferative drugs, hypersensitivity reactions to the polymer and metal, circulating levels of MMPs, low wall shear stress, polymer release kinetics have also been demonstrated to be contributive to ISR development

[60]. Further, different types of DES have also been shown to affect the phenotype of VSMCs with synthetic phenotype more frequent with BMS and paclitaxel-eluting stents (PES), intermediate with Zotarolimus-eluting stent (ZES) and Sirolimus-eluting stents (SES), contractile with tacrolimus-eluting stent (TES) [61].

Role of Endothelial Cells: Mechanical injury from coronary intervention leads to denudation of the endothelium and subsequently leads to a sequel of events resulting in VSMC migration and proliferation. Re-endothelialization is a critical step to completion of the wound healing response to PCI-induced injury of the vessel wall. Endothelial dysfunction is commonly observed at sites of regenerating endothelium. Studies with drugs that enhance endothelium-derived relaxing factors or diminish endothelium derived contracting factor production have been shown to control restenosis [62]. Further, the extent of the denuded area is also contributive to re-endothelialization and hence intimal hyperplasia as small denuded areas heal more quickly [63].

Role of Platelets, Macrophages and VSMCs: Proliferation and migration of vascular smooth muscle cells from the medial layer over time results in the formation of neointima. As described previously, increased trafficking of inflammatory cells and platelets at the site of injury leads to an increase in local concentration of growth factors and cytokines which stimulate phenotypic modulation of VSMCs possibly due to degradation of the basement membrane via MMPs secreted by macrophages.

Role of Hemodynamics: In stented vessels, low wall shear stress has been inversely correlated with neointimal thickening using 3D-reconstruction and finite element analysis [64, 65]. Further, Wenetzel et al also showed similar results in 14 patients after stent implantations in coronary arteries [66]. VSMCs respond to shear stress variations such that low wall shear stress is contributive to VSMC proliferation and hence neointima formation whereas high shear shows an opposite effect

[67].Further evidence exists in studies where reduced number of stent wires and strut thickness have resulted in less of vessel area exposed to low shear stress [68].

Classification of In-Stent Restenosis Lesions: Based on angiographic patterns, restenotic lesions have been classified as Focal (Type Ia or at articulation/gap, Ib or at stent margin, Ic or at focal body, Id or multifocal) and Diffuse (Type II, III and IV). Type I lesions are typically ≤ 10 mm in length and may be located at the unscaffolded segment (Type Ia) or at the body of the stent (Type Ib), proximal or distal margin of the stent (Type Ic) or combination of these sites (Type Id). Type II lesions or diffuse-intrastent are > 10 mm in length and are confined to the stented area without any distal or proximal extensions. Type III or diffuse proliferative are lesions > 10 mm in length and extend beyond the stent margin. Type IV or total occlusion represent lesions with no flow and require immediate revascularization [69].

Predictors of Restenosis: Three major classes of factors, which serve as predictors of restenosis, have been defined- Patient-related factors, Vessel-related predictors and Procedure-related factors. Various patient-related factors including high serum levels of C-reactive protein (CRP) & Interleukin-6 (IL-6), previous angioplasty. However, the most consistent patient-related factor is the presence of Diabetes with a 30-50% increased risk of developing restenosis. Vessel-related factors such as vessel diameter and lesion length independently serve to predict the incidence of in-stent restenosis with larger diameter/shorter lesions demonstrating significantly lower restenosis rates [70]. Finally, procedure-related factors such as stent-strut thickness, stent fracture, stent length and minimum lumen diameter serve as significant clinical predictors of restenosis [58]. Thinner-struts are hemodynamically more favorable as compared to thicker struts. With increase in stent length, rate of In-stent restenosis (ISR) have been reported to be nearly double for stent lengths > 35 mm [71].

1.1.6 *Vascular Smooth muscle cells biology:*

Vascular smooth muscle cells (VSMCs) are primarily responsible for establishing and orchestrating contraction and distension in blood vessels. VSMC maintain contractile tone by a highly organized architecture of contractile/cytoskeletal proteins and associated regulatory components within the cell cytoplasm and establish distensibility by synthesis, secretion and organization of the extracellular matrix (ECM) components with elastic recoil and resilience properties. The primary function of vascular smooth muscle cells is to maintain the vascular tone via contraction and dilation. VSMCs expresses a variety of contractile proteins, ion channels and signaling molecules that regulate its contraction. [72]. Upon contraction VSMCs shorten, thus decreasing the diameter of a blood vessel to regulate the blood flow and pressure. Changes in the cytosolic calcium ion concentration or [Ca^{2+}] are the principal mechanisms that regulate the contractile state of VSMCs [73].

The contractile proteins in a VSMC are packed into thin and thick filaments: thin filaments are composed of Actin, Tropomyosin and specific thin filament-binding proteins (e.g. caldesmon, Calponin), while the thick filaments are composed of myosin. Upon receiving contractile stimuli, there is an increase in the cytosolic calcium ion concentration [74]. When cytosolic [Ca^{2+}] exceeds 1 µM, calcium ions bind to calmodulin (CaM), with four calcium ions binding to each calmodulin, leading to a conformational change in CaM. In the altered conformational state, the $4Ca^{2+}$ - CaM complex binds to and activates myosin light-chain kinase (MLCK). The active kinase complex, $4Ca^{2+}$ - CaM – MLCK, subsequently phosphorylates myosin at 20-kD myosin light chain (MLC20) on serine 19 thus allowing myosin adenosine triphosphatase (ATPase) to be activated by actin which leads to contraction of the muscle as a result of MgATP-dependent cyclic interactions of myosin with actin [73, 75, 76]. The myosin molecules extend from the thick filaments to bind to actin via cross—bridges and on association with actin, myosin converts chemical energy (ATP) into movement of the heads (attached to actin) which exerts force on the thin actin filaments and causes shortening of the VSMCs [74]. However, when the cytosolic concentration of Ca^{2+} falls below 1

μM, due to the cellular extrusion or uptake by sarcoplasmic reticulum (SC), CaM dissociates from MLCK thus causing its inactivation. During these conditions, myosin phosphatase dephosphorylates MLC20 and leads to relaxation by inactivating actomysoin ATPase (actin-activated, ATPase activity of myosin). Dephosphorylating activity of myosin phosphatase is independent of the cytosolic [Ca^{2+}] [74].

VSMCs within the vascular continuum have the ability to adapt to extrinsic and intrinsic cues during different developmental stages and in disease response to an injury stimulus. This ability is due to a phenomenon known as the phenotypic modulation and is a major feature that distinguishes VSMCs from terminally differentiated skeletal muscle cells and cardiomyocytes [72].

Contractile phenotype: Contractile-state VSMCs are characterized by a range of contractile proteins, contractile-regulating proteins, contractile agonist receptors and signaling proteins responsible for contraction and maintenance of vascular tone. In addition, contractile smooth muscle cells (SMCs) are elongated, spindle –shaped cells in culture composed of tightly bundled myofilaments and minimal rough endoplasmic reticulum, Golgi or free ribosomes [72]. These cells exhibit a low proliferation index. The expression patterns of a wide range of protein markers have been characterized to describe the phenotypic state of SMCs. Since contractile SMCs exhibit a mature contractile apparatus, proteins, which are predominantly involved in SMC contraction, also serve as the contractile state markers. These include smooth muscle α-Actin (SMαA), smooth muscle myosin heavy chains SM-1 and SM-2, Calponin, SM-22α and Smoothelin and h-caldesmon [77]. In addition to contraction-related protein expression, contractile VSMCs exhibit differential levels of extracellular matrix (ECM) components (increased type I and IV collagen) and decreased matrix metalloproteinases (MMPs) and increased tissue inhibitors of MMPs (TIMPs) [72].

Synthetic/dedifferentiated: During non-pathological processes such as normal vascular development or upon injury VSMCs exhibit a dedifferentiated/synthetic phenotype, characterized by high rate of proliferation, migration and production of ECM components. Synthetic VSMCs also demonstrate a decreased expression of contractile-state associated proteins (SMMHC, SMαA, Calponin, SM-22α etc.) with concomitant increased expression of osteopontin, 1-caldesmon, non-muscle myosin heavy chain, vimentin, tropomyosin 4 and cellular-retinal binding-protein-1 (CRBP-1) [72]. Morphologically, synthetic VSMCs have increased cell size and exhibit hill-valley morphology in culture. Ultrastructure of these cells shows a cytoplasm devoid of contractile bundles with extensive rough endoplasmic reticulum, Golgi and ribosomes [78]. Phenotypic modulation of vascular smooth muscle cells plays a major role in development of progression of various diseases including Atherosclerosis, Hypertension, Vascular calcification and in the healing response to mechanical injury to the vessel wall [79].

1. Atherosclerosis: Vascular smooth muscle cell phenotypic modulation is a critical contributor to the development of atherosclerosis. Medial VSMCs are believed to undergo phenotypic modulation and migration into the intima, where they proliferate and secrete copious amounts of extracellular matrix and thus participate in fibrous cap formation [80]. In addition, a general consensus on increased VSMC content conferring atherosclerotic plaque stability also exists [79].

2. Systemic Hypertension: It is clinically defined as a sustained diastolic pressure of > 90 mmHg or systolic pressure > 120 mmHg. The exact mechanism of systemic hypertension is not completely known however a common feature is increase in the peripheral resistance, as a result of increased vascular tone/SMC contractility and vascular remodeling [81]. Increased intracellular calcium handling/release and changes in membrane polarizations have been shown to be contributive to increased contractility [81, 82].

3. Vascular Calcification: It involves increased levels of calcium deposition in major arteries resulting in an impaired vascular compliance and recoil in the aorta and muscular arteries in general and in response to balloon dilation [83, 84]. Vascular calcification promotes systolic hypertension, coronary insufficiency and intensifies cardiac energy demand. It also promotes ischemia and serves as a predictor for amputation [85]. Molecules that characteristically regulate osteoblast differentiation and bone formation including osteogenic transcription factor Runx2, osteopontin, osteocalcin, type I collagen and BMP-2 have been found in calcifying vessels [86, 87]. In the presence of increased phosphate levels, BMP-2 has been shown to increase phosphate transport across VSMCs in a dose-dependent manner, thus promoting osteogenic phenotypic transition of SMCs [88]. In addition, bovine aortic smooth muscle cells (BASMCs) have been demonstrated to loose contractile lineage markers after culturing in calcifying conditions [89].

4. Aneurysms: These are defined as a weak area in the wall of a blood vessel that leads to widening or ballooning of the artery. Studies have shown reduced expression of contractile-state markers in VSMCs and concomitant increase in MMP-2 and MMP-9 in animal models and human aneurysms. These events were shown to occur before the formation of aneurysms [90].

1.1.7 *Diabetes-related complications*

Diabetes remains the seventh leading cause of death in the United States with nearly 1.7 million new cases of diabetes are reported every year leading to a total economic burden of about $245 billion in direct and indirect healthcare costs [91]. Cardiovascular disease account for about 68% of diabetes-related deaths annually as patients with diabetes have a four to six-fold increased risk for

cardiovascular events in comparison to non-diabetic patients and appear to develop more severe coronary artery disease [92].

Pathology of diabetes and types

Diabetes encompasses a range of disorders like Type 1 Diabetes Mellitus (T1DM), type 2 diabetes mellitus (T2DM), gestational diabetes mellitus, drug-or chemical induced diabetes (for example from some second-generation antipsychotic drugs and some anti-human immunodeficiency virus (HIV) drugs as well as exposure to combination antiretroviral therapy) [93]. However, majority of the cases of diabetes are of type 2.

Type 1 diabetes is characterized by a long preclinical period of autoimmune attack on the beta cells, carried out by autoreactive T-cells and marked by the emergence of autoantibodies against β-cell autoantigens. Type 1 diabetic patients are unable to secrete insulin in response to a glucose load and thus eventually become hyperglycemic [94].

T2DM patients or non-insulin dependent diabetes is due to desensitization of insulin receptors. It develops slowly and at an early stage is characterized by the development of insulin resistance. This is associated with a reduction in glucose uptake by target cells and an altered lipid metabolism. Hyperinsulinemia, hyperglycemia and dyslipidemia area common features of T2DM and as the disease progresses, β-islet cell function becomes impaired and eventually fails, signaling the development of overt type 2 diabetes [95].

Diabetes and Atherosclerosis

The histological course of atherosclerosis in diabetes is nearly the same as for non-diabetic patients. However, atherosclerotic plaques in the presence of diabetes demonstrate higher levels of vascular calcification, greater number of necrotic cores, increased expression of receptor for advanced

glycation end-product (RAGE) on endothelial and smooth muscle cells and increased macrophage and T-cell infiltration [25]. Coronary atherectomy specimens collected from diabetic patients demonstrated that patients with diabetes exhibited a larger content of lipid-rich atheroma than those without diabetes [96]. In addition, carotid endarterectomy specimens from Type 2 diabetic patients were shown to be richer in macrophages and T-lymphocytes with increased expression NF-κB and MMPs [97].

Role of Dyslipidemia

Elevated triglycerides, reduced high density lipoprotein cholesterol (HDL-C) concentrations and elevated levels of free fatty acids (FFA) define the characteristic lipid profile in diabetic patients. Increased triglycerides can be attributed to a functional defect in the enzyme lipoprotein lipase which is involved in hydrolyzing fatty acids from triglycerides. A functional defect in the enzyme has been associated with diabetes thus leading to a decreased expression of apolipoprotein A-I and thus HDL particles. In addition, expression and activity of an endothelium bound phospholipase, endothelial lipase, is also involved in catabolizing HDL thus further reducing their level. Further, hepatic dysregulation as a consequence of a fatty liver, hyperinsulinemia, and hyperglycemia exacerbates the lipid metabolism. LDL particles in T2DM are considered to be more pathogenic since these particles are smaller, denser and hence more prone to entry, oxidation and retention in the blood vessel [98].

Elevated thrombotic response

Diabetes is associated with a pro-thrombotic state characterized by platelet hyperactivity, increased coagulation and impaired fibrinolysis [99]. High glucose has been reported to cause increased platelet reactivity by increased PKC activation followed by subsequent granule release & aggregation [100], non-enzymatic glycation of proteins on the surface of the platelets [101]. Further, hyperglycemia mediated redox imbalance leading to an increase in reactive oxygen species has been shown to affect the activity of calcium ATPases [102] thus increasing the intracellular calcium levels

in platelets and reducing cAMP levels consequently leading to an increased aggregation and activation of platelets. Increased activation of pro-thrombotic coagulation factors such tissue factor, Factor VII, XIII has been reported in T2DM [98].

Endothelial Dysfunction

The endothelial layer provides a physical barrier to blood flow from the vessel wall. It also controls homeostatic processes including blood pressure, hemostasis and homing of immune cells to the sites of inflammation. It produces mediators that induce vasoconstriction including endothelin, prostaglandins, and angiotensin II [103]. ECs produce nitric oxide using L-arginine by the action of eNOS in repose to blood flow changes [104]. The balance between vasodilation and vasoconstriction is fundamental to maintenance of the arterial pressure. In case of diabetic patients, metabolic complications like hyperglycemia, elevated free fatty acid levels, increased ROS production, insulin resistance lead to endothelial dysfunction which manifests as impairment of NO-dependent vasodilation [98]. Dysfunctional endothelial cells are associated with an increased adhesion of circulating leukocytes and platelets via upregulation of adhesion receptors and also exhibit an increased LDL permeability and retention thus contributing to the development of atherosclerosis in diabetes [103].

Role of Inflammatory cells

Type 1 diabetes has been shown to cause an increase in circulating inflammatory markers such as C-reactive protein, soluble intercellular adhesion molecules, CD 40 ligand [105-107]. In addition, T1D also promotes an increase in IL-6, Il-8, IL-1α. Further, release of saturated fatty acids also promote the release of pro-inflammatory cytokines by monocytes in case of T2D [107]. In animal models of atherosclerosis, hyperglycemia has been shown to accelerate influx of inflammatory markers through the TGF-β signaling pathway [108].

Role of Vascular Smooth muscle cell

Although the main role of VSMCs in atherosclerosis involves their phenotypic modulation, migration to suboptimal space, proliferation and extracellular matrix synthesis thereby enlarging the neointimal lesion. VSMCs grown in vitro under high glucose conditions demonstrated an increased proliferation, migration hypertrophy and higher ECM production in comparison to low glucose conditions [109, 110]. VSMC from diabetic mice exhibited an increased expression of proinflammatory gene expression including MCP-1 and IL-6 [111, 112]. Thus diabetic state predisposes VSMCs to the development of atherosclerosis.

Diabetes and Restenosis

The state of diabetes has been consistently reported as the main patient related risk factor for developing restenosis after PCI in various clinical trials. Van belle et al reported restenosis rates to be almost twice as much as in non-diabetic patients (63% vs. 36%) at 6 month follow up of balloon angioplasty. Initial observations correlated late vessel occlusion with increased restenosis in these patients however after excluding patients with late occlusion, restenosis rates were still higher in diabetic patients [113] suggesting involvement of additional mechanism such as negative remodeling acute recoil and greater neointimal response.

Clinical trials comparing restenosis rates between diabetic and non-diabetic patients have demonstrated higher rates of both angiographic restenosis (diameter stenosis $\geq$50% determined angiographically) [114-117] and clinical restenosis (requiring target lesion revascularization) [115, 118, 119]. As mentioned previously, restenosis after stent implantation is primarily due to an exaggerated neointimal hyperplasia and increased tissue proliferation has been reported with serial IVUS analysis in diabetic patients [120].

Use of first generation drug-eluting stents reduced the overall rates of restenosis when compared to bare-metal stents alone in all patients including those affected by diabetes [121-123]. However, emergence of stent thrombosis became a safety concern with these devices. Studies have reported a

significant difference in the survival rate favoring BMS over Sirolimus eluting stent (SES) with a lower survival rate for patients with diabetes. This difference was not observed in patients without diabetes [124] with additional evidence from studies reporting higher death rates due to cardiac causes in diabetic patients treated with SES [125]. As compared to SES, paclitaxel eluting stents have been reported to have higher cases of Stent thrombosis in diabetic patients at 1 year [126, 127]. In addition, rates of restenosis remained highest for diabetic patients requiring insulin treatment, irrespective of stent type [128]. Second-generation of drug eluting stents had an optimized drug deliverability while seeking to minimize target lesion revascularization (TLR) and ST. A summary of clinical trials comparing the efficacy of different DES in diabetic patients are listed in table 1 [1]. Diabetic patients still represent a high risk patient population with patients requiring insulin therapy being the most affected [1].

Trial	Conclusion
SYNTAX (TAXUS) [129]	Increased MACE (Major adverse cardiac events) after PCI
FREEDOM [2] (TAXUS) [130]	CABG (Coronary artery bypass grafting) better for all cause morality, MI (Myocardial Infarction), stroke
SPIRIT V [3] (Xience V vs TAXUS) [131]	Paclitaxel-eluting stents (PES) increased In-stent late loss
Pooled analysis of SPIRIT II,III,IV and COMPARE [4] (TAXUS) vs. Xience V EES [132]	**No difference** in safety or efficacy of Endeavor Everolimus-eluting stents (EES) vs. PES **in diabetic patients** when EES led to decreased mortality, MI, ST (Stent thrombosis) and TLR (Target-lesion revascularization) in non-diabetic patients.
ENDEAVOR IV [133]	**In-stent restenosis (%) increased** in patients with Diabetes treated with E-ZES (Zotarolimus-Eluting Stent).
E-FIVE [134]	Diabetic Patients had **significantly higher rates** of **MACE**, **TLR**, **TVF** (**Target vessel failure)** and **ST** as compared to non-diabetic at 1 year.
NAPLES-DIABETES [135]	E-ZES led to **increased** 3 year rates of **MACE** due to **higher** rates of **TLR**.
Pooled Analysis of International global RESOLUTE program [136]	Insulin treated patients affected by significantly high Target lesion failure (13.7%).

Table 1.1: List of clinical trials comparing efficacy of drug eluting stents in diabetic patients [1].

Characterization of restenotic lesions at 1 year after DES implantation by optical coherence tomography revealed thicker neointima in case of diabetic patients with direct correlation of glycemic control (HbA_{1C} levels) and neointimal thickness. Further, incidence of low signal pattern in poor glycemic control group was significantly higher thus demonstrating large amounts of extracellular matrix and proteoglycans in these lesions [137] eventually increasing the risk of stent thrombosis [1].

Contribution of Hyperglycemia

Evidence for contribution of hyperglycemia to development of restenosis comes from clinical studies demonstrating a poor glycemic control associated with increased restenosis due to higher rates of target lesion revascularization. In addition to long-term glycemic control, pre-procedure hyperglycemia has been demonstrated to be strongly correlated with restenosis in diabetic patients since diabetic patients with pre-procedure hyperglycemia (> 128 mg/dl) had a 33.8% target-vessel revascularization (TVR) rate at 9-month follow up [138, 139]. Furthermore, pre-procedural hyperglycemia was independent of glycated-hemoglobin (HbA_{1C}) levels as diabetic patients with $HbA_{1C} \leq 7\%$ but pre-procedure glucose levels > 128 mg/dL had significantly higher rates of TVR as compared to $HbA_{1C} \leq 7\%$ & pre-procedure glucose < 128 mg/dL [140]. Similar results were found by Nusca et al where pre-procedure hyperglycemia was correlated with increased rates of target vessel failure (TVF) [141]. Hyperglycemia may mediate these effects via differential response of various cellular components involved in development and progression of neointimal hyperplasia and our current understanding of these remains less well understood.

Mechanism of restenosis involves denudation of the endothelium followed by attachment of platelets and inflammatory cells at the site of injury which leads to an increase in local growth factors and inflammatory markers thus affecting VSMC migration and proliferation. Hyperglycemia has been shown to affect all of these processes.

Hyperglycemia has been shown to increase activation and aggregation of platelets via increase in PKC activation [100], direct osmotic effects [142] and by induction of non-enzymatic glycation of platelet-surface proteins [143]. In addition, acute hyperglycemia has been shown to cause an increased expression of P-selectin and CD40 ligands by platelets [144, 145]. Further, hyperglycemia mediated advanced glycated-end products (AGE) & reactive oxygen species (ROS) production can lead to elevated expression of procoagulant tissue factor by endothelial cells via activation of NF-κB [146]. This mechanism also plays an important role in hyperglycemia mediated reduction in tissue p[plasminogen activator (t-PA), ultimately promoting thrombosis [147].

As a part of vascular healing, endothelial progenitor cells (EPC) have been demonstrated to play an important role in re-endothelialization of blood vessels post injury with studies demonstrating the approach of capturing circulating EPCs contributive to accelerated re-endothelialization [65]. Diabetes has been related to delayed re-endothelialization in animal models [148]. Human EPC subjected to high glucose (12.5 mM) have been shown to induce senescence via phosphorylation p38 MAPK [149] thus serving as a potential mechanism for impaired re-endothelialization associated with diabetes.

Vascular smooth muscle cell migration and proliferation in the intima is a key event in the development of neointimal hyperplasia and restenosis. Significant in vitro evidence exists on direct effects of high glucose in causing vascular smooth muscle proliferation via upregulation of growth factors such basic FGF (bFGF), Transforming growth factor alpha (TGF-α) [150, 151], upregulation of osteopontin release [152] , increased polyol pathway flux [153], upregulation of protein kinase C [154], increased DNA synthesis [155], increased IGF-1 responsiveness resulting in enhanced proliferation and migration [156], suppression of AMP activated protein kinase (AMPK) resulting in activation of mammalian target of rapamycin (mTOR) [157, 158], upregulation of MAPK, PI3K/Akt and NF-κB [159]. In addition animal models of type 2 diabetes reported a significantly higher cell proliferation at 3 days post arterial injury as compared to controls [160]. Although

contradictory results have been reported in models of type I diabetes with no difference [161] and significant difference in contribution of hyperglycemia to neointimal thickness [162], these differences have been attributed to the extent of streptozotocin treatment. Thus, hyperglycemia independently may contribute to neointimal hyperplasia [153]. Additionally, hyperglycemia has also been reported to increase SMC migration via PKC dependent pathway [163].

1.2 Clinical Significance:

Diabetes represents one of the major global health issues with nearly 1.7 million new cases reported each year. These patients are at a four-to-six fold increased risk of developing cardiovascular diseases with reports of up to 68% of deaths associated with it. Diabetic patients are more vulnerable to restenosis due to a greater need for revascularization. However, prognosis of PCI in diabetic patients remains consistently poor with the state of diabetes being the most consistent patient-specific predictor of developing Restenosis. Major advances in stent technology, with the advent of drug-eluting stents, have reduced the overall rates of restenosis when compared to bare-metal stent alone however restenosis rates for diabetic patients are still higher when compared to their non-diabetic counterparts.

Development of restenosis post-angioplasty is primarily due to negative recoil of the blood vessel in response to balloon distension. Restenosis after implantation of stents is primarily due to the development of Neointimal hyperplasia (NIH). The exact mechanisms that trigger NIH are not completely understood however phenotypic modulation of vascular smooth muscle cells plays a key role in the development of neo-intima.

Vascular smooth muscle cells possess a unique characteristic of switching their phenotype in response to the external stimulus. Although the plasticity exhibited by these cells is critical for wound healing, this remarkable capacity of the cells is also contributive to the development of cardiovascular diseases such Atherosclerosis, Vascular calcification, Aneurysms, Hypertension and

Restenosis. Exposure to a stimulus, leads to dedifferentiation of smooth muscle cells from a contractile/quiescent state to a synthetic state. Synthetic smooth muscle cells are characterized by their higher rate of proliferation, increased migratory capacity, loss of contractile-state associated proteins, increased synthesis of extracellular matrix molecules, increased expression of matrix metalloproteinases, and increased expression of osteoblast-like cell markers. Mechanical injury from PCI procedures have shown to cause denudation of the endothelium thus exposing medial smooth muscle cells to shear forces from blood flow in addition to a myriad of circulating growth factors. These events signal medial smooth muscle cells to dedifferentiate into a synthetic phenotype, migrate to the intima and proliferate.

Although the contribution of phenotypic modulation to the development of restenosis has been well explored nevertheless, our understanding of this characteristic response in diabetic patients remains less understood. The current study attempts to further our understanding in this domain and proposes a dynamic-disease model to explore the influence of diabetes-related hyperglycemia on phenotypic modulation of smooth muscle cells by subjecting SMCs to clinically relevant mechanical forces in the presence of high glucose conditions.

1.3 Project Aim:

This study was aimed at developing an *In Vitro* disease model to compare vascular smooth muscle cell response to two clinically relevant pathological stimuli- Low wall shear stress and Hyperglycemia. As a secondary aim, we also compared VSMC response in acute hyperglycemic condition with long-term conditioned chronic hyperglycemia when subjected to cyclic strain and low wall shear stress.

Chapter 2

"Effects of clinically relevant mechanical forces on hyperglycemic vascular smooth muscle cells: An *In Vitro* Dynamic Disease Model"

2.1 Introduction:

Cardiovascular diseases account for about 68% of diabetes-related deaths and with nearly 1.7 million new cases of diabetes reported each year resulting in considerably high economic burden [3]. Patients with diabetes have a four to six-fold increased risk for cardiovascular events in comparison to non-diabetic patients and appear to develop more severe coronary artery disease [92]. Outcomes of percutaneous coronary interventions (PCI) have been reported to be less favorable in case of diabetic patients [113, 164]. The increased risk of restenosis in diabetic patients has been attributed to an exaggerated intimal hyperplasia eventually leading to a greater late lumen loss and decreased vessel lumen area [120]. Drug eluting stents have successfully reduced the overall rates of restenosis however diabetic population remains at a higher risk group with reports demonstrating higher rates of restenosis associated with diabetes [165].

Barotrauma from a percutaneous coronary intervention (PCI) causes endothelial denudation and consequently exposes underlying smooth muscle cells to a myriad of circulating growth factors and promotes a phenotypic shift of vascular smooth muscle cells (VSMCs) from contractile to synthetic state, which is characterized by an increased capacity of VSMCs to migrate and proliferate from the medial layer to form the neointima followed by increased secretion of extracellular matrix [166]. Phenotypic modulation is considered to be one of the key mechanisms responsible for initiation and progression of neointimal hyperplasia and restenosis. In addition to growth factors, hemodynamic forces such as wall shear stress from blood flow and cyclic strain also control the phenotype and function of VSMCs [167]. Physiological levels of cyclic strain ($\leq$ 10%, 1Hz) mimicking an *in vivo* environment have been shown to promote quiescent, contractile phenotype of VSMCs [168] in contrast to high strain rates which have been shown to promote SMC proliferation and

dedifferentiation [169-171]. In case of endothelial injury or vascular smooth muscle cell migration into the intima, blood flow may directly act on the superficial layer of VSMCs [167]. Shear forces have been shown to have direct effects on phenotypic modulation of vascular smooth muscle cells with physiological shear stress (5-25 dynes.cm^{-2}) reducing proliferation and promoting contractile phenotype [172, 173] and low wall shear stress leading to SMC proliferation [174] and migration via upregulation of platelet-derived growth factor (PDGF) [175]. Additionally, *in vivo* and clinical studies have demonstrated areas of low wall shear stress to be associated with thicker neointima [176, 177].

Hyperglycemia is the hallmark of diabetes with clinical evidence of its association with higher rates of target lesion revascularization (TLR) amongst diabetic patients [138, 139]. Furthermore, preprocedure hyperglycemia, independent of glycated hemoglobin (HbA_{1C}), has been demonstrated to be strongly correlated with restenosis in diabetic patients [140]. Contributive effects of hyperglycemia in neointimal thickening have also been demonstrated in animal models of type I diabetes [162]. At a cellular level, exposure of SMCs to high glucose conditions has been demonstrated to show hyperproliferation [154, 178-180], hypertrophy [154] and enhanced migration [181, 182].

Although various studies have implicated a pro-restenotic response of VSMCs to hyperglycemia, cellular response to hyperglycemia in combination to mechanical forces and thus injury-mediated response in diabetic patients is not completely understood. Thus, we hypothesize that exposure of clinically relevant mechanical forces under chronic hyperglycemic conditions will lead to a greater phenotypic modulation of vascular smooth muscle cells. Further, results from the current study will be compared to prior art in order to determine the relevance of our dynamic disease model.

2.2 Materials and Methods:

Cells cultured on type-1 collagen coated silicone membrane were subjected to static-control (U) or Cyclic Tensile (CT) stress or cyclic tensile and low wall shear stress (CTS). Mechanical loading was performed on a previously designed custom simulator set up, which enables application of cyclic tensile stress and low wall shear stress on cultured cells. Cells were subjected to either physiological cyclic strain (0-7%) at 1 Hz for 24 hours (CT) or to cyclic tensile strain and low wall shear stress (CTS, ~0.30 dynes.cm^{-2}) from externally supplied flow at 350 mL/min using a peristaltic pump for 24 hours (CTS). Cyclic strain was applied using FlexCell-3000™ system (Flexcell International, NC). Cells cultured on type-1 collagen coated silicone membranes in a 12-well plate served as static controls (U). All experimental groups are summarized in table 2.1.

	Unloaded/Static	**Cyclic Tensile**	**Cyclic Tensile + Shear**
Low glucose	**LG U:** Cells subjected to 5.5 mM D-glucose	**LG CT:** Cells subjected to 5.5 mM D-glucose under cyclic strain (0-7% at 1Hz, 24 hr)	**LG CTS**: Cells subjected to 5.5 mM D-glucose under cyclic strain (0-7% at 1Hz) and shear from flow (~ 0.3 dynes.cm^{-2})
Acute high glucose	**AG U:** Cells subjected to 25 mM D-glucose for 84 hours	**AG CT:** Cells subjected to 25 mM D-glucose for 84 hours (36 hrs. seeding + 24hrs. quiescence + 24 hrs. loading) under cyclic strain loading (0-7% at, 1Hz, 24hr)	**AG CTS**: Cells subjected to 25 mM D-glucose for 84 hours under cyclic strain (0-7% at 1Hz) and shear from flow loading(~ 0.3 dynes.cm^{-2})
Chronic high glucose	**CG U:** Cells acclimated to 25 mM D-glucose for 3-4 weeks before testing and during mechanical loading	**CG CT:** Cells acclimated to 25 mM D-glucose for 3-4 weeks before testing and during mechanical loading under cyclic strain loading (0-7% at 1Hz)	**CG CTS**: Cells acclimated to 25 mM D-glucose for 3-4 weeks before testing and during mechanical loading under cyclic strain (0-7% at 1Hz) and shear from flow loading (~ 0.3 dynes.cm^{-2})

Table 2.1*: Experimental group summary*

Cell Culture and Characterization:

Fresh aorta from female Sprague-Dawley™ rats (8-10 weeks old) were obtained and were enzymatically digested to isolate smooth muscle cells in a modified two-step digestion method [183] (approved by Clemson University Institutional Animal Care and Use Committee). Briefly, isolated aorta was first treated with Dulbecco's modified eagle medium MEM (5.5 mM, Corning 10-014-CV or 25 mM D-Glucose, Corning 10-013-CM) containing collagenase type-II (300U/mL, Worthington 4176) and 1% antibiotic/antimycotic (Penicillin/streptomycin, Cellgro 30-004-CI) at 37^0C for 15 minutes. This pretreatment with collagenase type-II enables easier removal of adventitia without overstretching the aorta. At the end of incubation, adventitial layer of aorta was removed under sterile conditions. Next, the aorta was split open longitudinally and its luminal surface was gently scrapped off to remove endothelial cells and finally was rinsed in PBS at 37^0C (Corning 46-013-CM). Medial tissue was chopped into small squares (~1 mm wide) and transferred to the digestion solution (DMEM +1% Ab/m with 5.5 mM or 25 mM D-Glucose) containing collagenase type-II (300 U/mL) and elastase (10 U/mL, Worthington 2292). Digestion solution containing tissue was transferred to a 6-well plate and incubated at 37^0C for about 2 hours with gentle intermittent shaking at every 30 minutes for 5 minutes. After incubation, the digestion solution was centrifuged at 1000 rpm for 5 minutes, the supernatant was aspirated and pellet was re-dissolved in DMEM (5.5 mM or 25 mM D-Glucose) containing 10% fetal bovine serum ( ) and 1% Ab/m. Cells were cultured in DMEM containing normal (5.5 mM D-Glucose, LG) or high (25 mM D-Glucose, CG) until passage 6. Media was replaced every third day and cells became confluent every 10 days, beyond which they were passaged.

Characterization of smooth muscle cells was performed by immunofluorescence staining for α-SM actin. Briefly, cells were fixed with ice-cold fixative [4% paraformaldehyde, 0.1% glutaraldehyde and 4% sucrose in calcium magnesium free PBS (Mediatech, CM-PBS)] and were subsequently treated with blocking solution [3% bovine serum albumin (Santa Cruz 9048-46-8), 3% Goat Serum (Sigma, G9023)] and 0.1% Triton X-100 (Sigma, T-8787) in CM-PBS). After wash cycles, cells

were incubated overnight at 4^0C with anti-SM alpha actin antibody (ab 7817, Abcam) diluted to 1:100 in 3% BSA/PBS solution. After subsequent wash steps, cells were incubated with fluorescently tagged secondary antibody (A-11001, Life Technologies, diluted to 1:1000 in 3%BSA/PBS solution) for 1 hour. Cellular nuclei were stained with DAPI (Molecular Probes, A-21207, diluted to 1:3000 in PBS). Greater than 90% of the cells demonstrated to be α-SM actin positive.

Cell Seeding and Application of Mechanical Force:

For each experimental simulation, silicone membranes (diameter–6 cm) were cut from biomedical-grade silicone sheets of 0.015 inch thickness and 40 durometer hardness (SMI, 0.15" NRV G/G 40D). These were cleaned by sonication in deionized water and then autoclaved. A sterile station plate sandwich was formed using sterile station-rings and silicone membranes (Figure 2.1).

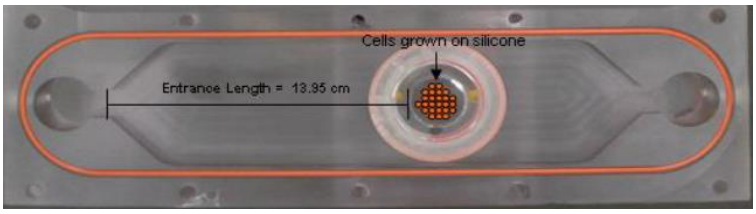

***Figure 2.1**: Loading station with plate sandwich at center*

The simulator design enables users to accommodate three of such assemblies on each baseplate (3 loading stations per baseplate, figure 2.2a) and with two baseplate it provides a total sample size of 6. Each sandwich assembly was placed on a loading post with 0.2 cc of silicone lubricant (Loctite, 51360) distributed evenly in between. Baseplate assembly was then UV-sterilized for 12 hours following which sterile Teflon rings (2.75 cm^2 inner cross-sectional area and 1.2 cm height) were centered on the silicone surface exactly above the loading post. The surface area confined using the Teflon ring was then coated with collagen type-I (Advanced Biomatrix, 5005B) at a final concentration of 50 µg/mL using deionized water [184].

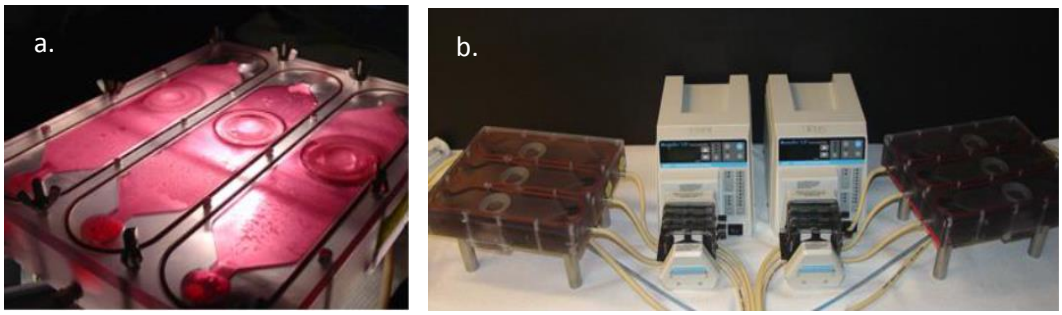

Figure 2.2: *a. Baseplate with 3 loading stations; b. External fluid supply with peristaltic pumps station with plate sandwich at center*

Prior to cell seeding, each collagen coated silicone membrane assembly was rinsed with 1 mL of DPBS (Cellgro, 21-031-CV). P2-P5 VSMCs were trypsinized (Corning, 25-050-CI) and counted using scepter cell-counter (Millipore, PHCC00000) and seeded at a density of 1.8×10^4 cells/cm ^{2} or 50,000 cells per well/loading station and allowed to attach and spread for 36 hours in media (5.5 mM or 25 mM D-Glucose) containing 10% FBS and 1% Ab/Am at 37 ^{0}C. After 36 hours, media was changed to DMEM (5.5 mM or 25 mM D-Glucose) containing 1% fetal bovine serum, 1% Ab/m and 1% Dextran (Sigma, 9004-54-0) to induce quiescence and adjust media viscosity respectively [184].

Cells were subjected to either physiological cyclic strain (0-7%) at 1 Hz for 24 hours (CT) or to cyclic tensile strain and low wall shear stress (CTS, ~0.30 dynes.cm^{-2}) from externally supplied flow at 350 mL/min using a peristaltic pump for 24 hours (CTS) (Figure 2.2b).

Cells cultured in high glucose conditions (25 mM) represented acute hyperglycemia (AG). AG cells were subjected to mechanical loading with cyclic tensile (CT) and cyclic-tensile shear (CTS) for 24 hours. Low glucose (5.5 mM) conditioned cells served as controls (LG). In addition, we also wanted to evaluate the phenotypic response of cells when preconditioned to high glucose conditions.

Represented by chronic hyperglycemia (CG), this group was incorporated to analyze the phenotypic differences attributable to prolonged high glucose exposure.

Cell Proliferation:

Proliferative capacity of the cells was analyzed using a CyQuant proliferation assay kit (Promega, 7026) using the manufacturer's protocol. Briefly, cells were trypsinized from the silicone membrane post simulation. Cell pellets were collected and frozen at -70 ^{0}C. On the day of the assay, pellets were thawed at room temperature and resuspended in 200 µL of 1x-lysis buffer containing GR-CyQuant dye at a final dilution of 80-fold. Each of the 200 µL samples were transferred to 96-black well plate and their fluorescence were recorded at an absorbance and emission maximum of 480 and 520 nm respectively with a microplate reader (Gen 5, Biotek Synergy 4). Cell counts were estimated using a fluorescence and known cell count standard curve for a sample size of 6 per treatment.

Apoptosis:

Cell apoptosis was measured using the Dead-End Tunel assay kit (Promega, G3250) using the manufacturer's protocol. This assay measures the fragmented DNA of apoptotic cells by catalytically incorporating fluorescin-12-dUTP at 3'-OH DNA ends using enzyme Terminal deoxynucleotidyl Transferase (rTdT) which forms a polymeric tail by nick end labeling. Briefly, cells were fixed with ice-cold fixative solution after each simulation for 15 minutes. Cells were then rinsed with 1x DPBS three times for 5 minutes per wash. Cells were permeabilized using 0.2 % triton X-100 (Fisher Bioreagents, 9002-93-1) in PBS for 5 minutes followed by three PBS rinses. Cells were then covered with 100 µL of equilibration buffer at room temperature for 10 minutes. After removing the equilibration buffer, 50 µL of the TdT reaction mix (45 µL equilibration buffer, 5 µL nucleotide mix and 1 µL rTdT Enzyme) was used to cover the cells. In order to prevent reaction mix from drying out, small silicone membranes were used to cover the cells without any bubbles. Membranes were then incubated at 37^{0}C in a humidified chamber without any exposure to light. The reaction was stopped with 2x SSC buffer after 60 minutes of incubation. Finally, silicone

membranes were washed in PBS three times, 5 minutes per wash. Counterstaining was performed with propidium iodide (Sigma, P4864) or Phalloidin (P1951, Sigma) diluted to 1:1000 in PBS. TUNEL positive cells were observed with a fluorescent microscope (Digital inverted microscope, EVOS f1, AMG). Cells were imaged with three random field-of-view per sample with apoptotic and total number cells emitting green and red fluorescence respectively. Percentage of apoptotic cells [(Tunel positive cells/total cells)*100] was determined for each sample and was averaged for across each treatment with total sample size of 18 per treatment.

Cellular Hypertrophy:

Cells after each treatment were fixed with ice-cold 4% fixative solution for 15 minutes followed by rinsing with PBS and permeabilization with 0.2% Triton X-100 in PBS for 5 minutes. Subsequent washes with PBS were done, following which cells were incubated with rhodamine-phalloidin (P1951, Sigma) diluted to 1:1000 in PBS. After 15 minutes, cells were rinsed with PBS and were incubated with 1:2000 DAPI in PBS. Finally cells were imaged using fluorescent microscope (Digital inverted microscope, EVOS f1, AMG). For each sample, five to six random field-of-view were recorded and analyzed per sample resulting in a total sample size of 125 per treatment. Cell area and aspect ratio were measured using ImageJ software (NIH). Mean cell area (μm^2) & aspect ratio (ratio of major axis length to minor axis length) were measured and analyzed for a sample size of 125 per treatment.

Protein Expression:

Quantification of contractile-state associated protein markers was performed using western blot. Briefly, protein was extracted from each sample using extraction buffer (10 µL/mL protease inhibitor cocktail, Sigma P 8340). Lysates were centrifuged at 14000g for 20 minutes at 4^0C, after which the supernatant was carefully removed and collected in fresh pre-chilled tubes. Total protein concentration was calculated using BCA-assay kit (Life Technologies, 23225) using BSA know

standards as described by manufacturer. For each lane 8 µg of protein was loaded on a 12% Tris-SDS acrylamide gels under denaturing conditions. Electrophoresis was performed for 120 minutes at 100 V. PVDF membranes were used to blot the proteins at 100 V for 75 minutes. Blots were subsequently blocked in 3% BSA in PBS solution for 1 hour at room temperature. Blots were incubated overnight at 4^0C with respective primary antibody (SM α-actin ab 7817, 1:500; Calponin, ab 46794, 1:2000; SM-22α, ab10135 1:1500; α-tubulin, ab7291 1:2500), diluted in 3% bovine serum albumin blocking buffer . After subsequent wash steps, blots were incubated with respective horse-radish peroxidase (HRP) conjugated secondary antibody (1:5000 Anti-rabbit; 1:7500 Anti-goat; 1:10000 anti-mouse) for 90 minutes at room temperature. Chemiluminescence substrate (Santa Cruz, SC-2048) was added prior to imaging of the blots and images were captured at approximately five minutes exposure setting. Densitometric analysis of the blots was performed with ImageJ software and α-tubulin served a loading control across all samples with a sample size of 6 per treatment.

Statistical Analysis:

Statistical Analysis was performed with One-way ANOVA and Tukey's post hoc for all data sets. All tests were performed with Minitab® 17 (Minitab Inc.)

2.3 Results:

Smooth muscle cell characterization:

More than 90% of the rat aortic smooth muscle cells, isolated from Spargue-Dawley™ rats by the described method, stained positive for SM α-actin as observed by Immunofluorescence (Figure 2.3).

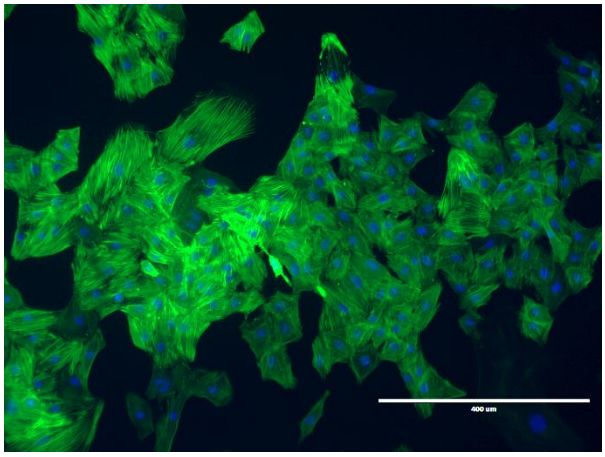

Figure 2.3: *Immunofluorescence staining for SM α-actin at passage 4. Nuclei were stained with DAPI. Image was captured at 100x magnification. Scale bar represents 400 µm.*

Cell Proliferation: Cell number estimation was performed using the CyQuant cell proliferation assay. Results from CyQuant showed 40213 ± 5010 cells in LG U, 60301 ± 3568 cells in AG U, 62472 ± 4593 cells in CG U, 28641 ± 2861 cells in LG CT, 44592 ± 5089 cells in AG CT, 33026 ± 3455 cells in CG CT, 41625 ± 6500 cells in LG CTS, 58932 ± 5712 cells in AG CTS and 56137 ± 1694 cells in CG CTS. Due to different glycemic levels (figure 2.4A), acute hyperglycemic cells demonstrated a significantly higher cell count as compared to low glucose controls under all mechanical conditions (p-value < 0.0001 for U, CT and CTS). Under chronic hyperglycemia, cell number increase was observed for all the loading conditions however significant differences were only observed for unloaded controls (p-value < 0.0001) and CTS samples ($p < 0.0001$). When comparing between different loading conditions (figure 2.4B), application of cyclic tensile led to a significant decrease in proliferation for all glycemic groups ($p = 0.0017$ for LG, $p < 0.0001$ for AG and CG). In addition, application of concomitant shear led to an increase in proliferation when compared to respective cyclic tensile condition for all low, acute and chronic high glucose ($p = 0.0003$ for LG, $p < 0.0001$ for AG and CG). Difference in cell proliferation between unloaded conditions and CTS were non-significant. All statistical comparisons were performed using ANOVA and Tukey's LSD method. Data values are summarized in table 2.2.

Sample	Unloaded (U)	Cyclic Tensile (CT)	Cyclic Tensile + Shear (CTS)
Low glucose (LG)	40213 ± 5010 cells	28641 ± 2861 cells	41625 ± 6500
Acute high (AG)	60301 ± 3568 cells	44592 ± 5089 cells	58932 ± 5712
Chronic high (CG)	62472 ± 4593 cells	33026 ± 3455 cells	56137 ± 1694 cells

***Table 2.2**: Data values for CyQUANT Assay (Cells count represented as Mean ± SD), n=6*

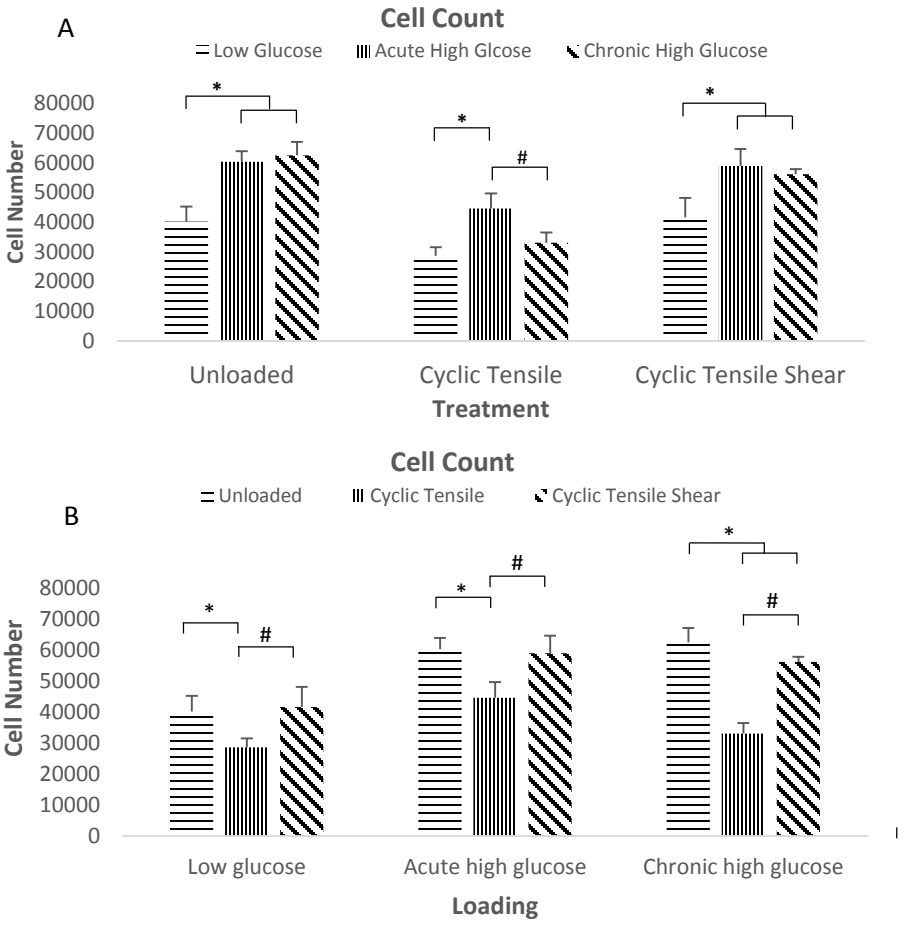

***Figure 2.4:** Values represented as Mean ± SD (error bar) with n = 6 for each sample. A). '*' represents p-value < 0.05 when compared to low glucose controls within each simulation group. '#' represents p-value < 0.05 for chronic samples when compared to acute high glucose samples within each simulation group. B). '*' represents p-value < 0.05 when compared to unloaded simulation, '#' represents p-value < 0.05 for cyclic-tensile shear samples when compared to cyclic tensile simulation for each glycemic group. All comparison performed with One-way ANOVA & Tukey post-hoc analysis.*

Apoptosis:

Images captured for each sample are represented in figure 2.5. Green fluorescence represents TUNEL positive cells whereas red fluorescence represents total cells in the respective field-of-view. For each field, both TUNEL positive cells and total number of cells were counted to estimate the percent apoptosis (TUNEL positive/Total number of cells *100) within each sample. Results from dead-end TUNEL assay (Figure 2.6) showed the ratio of apoptotic cells to total number of cells to be 1.74 ± 0.32% in LG U, in 7.84 ± 2.66% AG U, 8.31 ± 4.48% in CG U, 1.41 ± 0.67% in LG CT, 4.35 ± 1.10% in AG CT, 17.65 ± 2.06% in CG CT, 9.2 ± 5.26% in LG CTS, 12.23 ± 3.55% in AG CTS and 20.85 ± 3.55% in CG CTS samples. Data values are summarized in table 2.3.

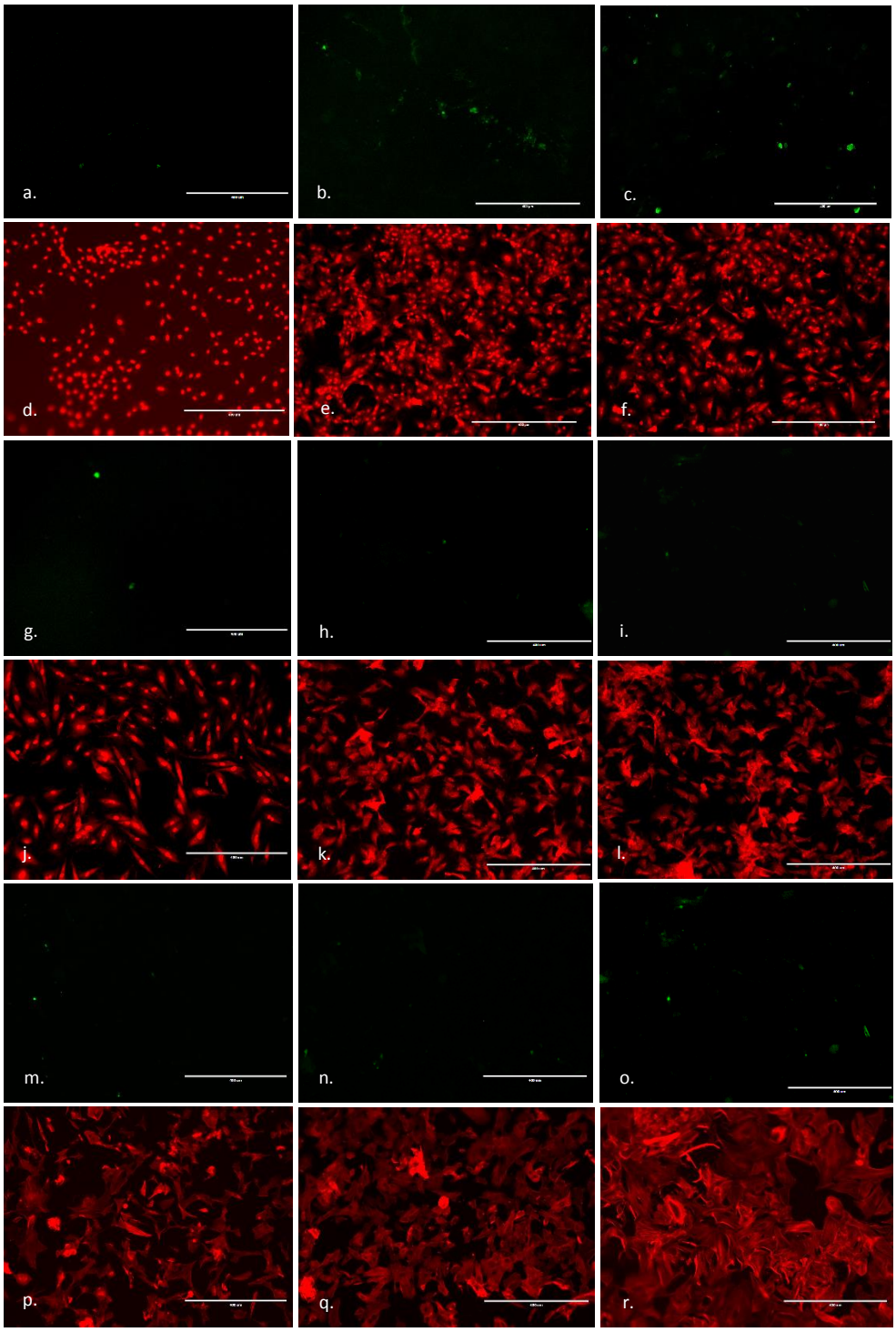

Figure 2.5: *Tunel Images for Low Glucose (left column), Acute High Glucose (Center Column) and Chronic High glucose (Right Column) with Unloaded (a-f), Cyclic Tensile (g-l) and Cyclic Tensile Shear (m-r). Green fluorescence represents Tunel labeled DNA fragments and red fluorescence represents counterstain at 100x magnification, Scale bar-400 µm*

Under acute hyperglycemia (figure 2.6A), VSMCs exhibited an increased number of apoptotic cells when compared to LG controls for unloaded conditions (p-value < 0.0001) and loaded conditions however, in case of mechanically loaded conditions statistical significance could not be achieved (p-value = 0.1 for CT, p-value = 0.08 for CTS). Similarly, chronic samples demonstrated a significantly higher number of apoptotic cells across all loading conditions in comparison to low glucose controls (p-value < 0.0001 for U, CT and CTS). Interestingly, chronic hyperglycemia led to an even higher number of apoptotic cells than acute hyperglycemia when subjected to mechanical loading in comparison to unloaded controls (p-value = 0.0001 for CT and CTS).

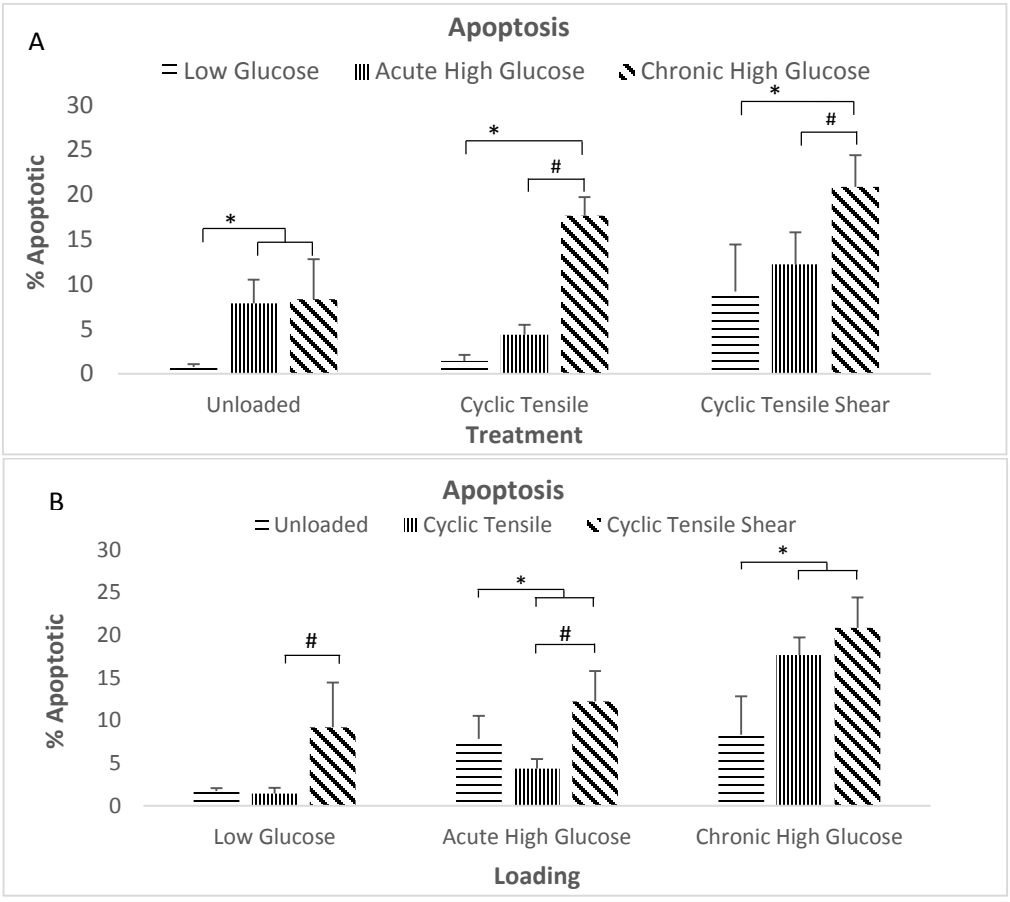

Figure 2.6: *Values represented as Mean ± SD (error bar) with n = 18 for each sample. A). '*' represents p-value < 0.05 when compared to low glucose controls within each simulation group. '#' represents p-value < 0.05 for chronic samples when compared to acute high glucose samples within each simulation group. B). '*' represents p-value < 0.05 when compared to unloaded simulation, '#' represents p-value < 0.05 for cyclic-tensile shear samples when compared to cyclic tensile simulation for each glycemic group. All comparison performed with One-way ANOVA & Tukey post-hoc analysis.*

Sample	Unloaded (U)	Cyclic Tensile (CT)	Cyclic Tensile + Shear (CTS)
Low glucose (LG)	0.74 ± 0.32%	1.41 ± 0.67%	9.2 ± 5.26%
Acute high (AG)	7.84 ± 2.66%	4.35 ± 1.10%	12.23 ± 3.55%
Chronic high (CG)	8.31 ± 4.48%	17.65 ± 2.06%	20.85 ± 3.55%

Table 2.3*: Data values for DeadEnd-TUNEL Assay (% Apoptotic Cells represented as Mean ± SD), n=18*

When comparing between different loading conditions (figure 2.6B), application of cyclic tensile led to a significant increase only for chronic high glucose treatment ($p < 0.0001$) in comparison to respective unloaded control. In contrast, application of cyclic tensile led to a decrease in percent apoptosis ($p = 0.0247$). Application of concomitant shear led to an increase in apoptosis when compared to respective cyclic tensile condition for all low and acute high glucose ($p < 0.0001$ for LG, $p < 0.0001$ for AG) with non-significant difference for chronic high glucose ($p =0.0560$). In comparison to unloaded conditions, application of CTS led to an increase in apoptosis for low ($p < 0.0001$), acute ($p <0.0012$) and chronic ($p < 0.0001$) treatment.

Cellular Hypertrophy:

Rhodamine-phalloidin was used to stain the F-actin fibers of VSMCs for each sample. Images were counterstained with DAPI and were captured using a fluorescent microscope (figure 2.7). Images for respective glycemic group are arranged column-wise with LG in left, AG in center and CG at right. Different rows represent mechanical loading conditions with unloaded in the top, cyclic tensile in the center and cyclic-tensile shear in the bottom row. From these images, it can be clearly appreciated that hyperglycemia led to an increase in cellular hypertrophy since low glucose sample appear to have more elongated morphology. For each sample, five to six random field-of-view were recorded and analyzed per sample resulting in a total sample size of 125 per treatment. Mean of cell area was observed to be 4003 ± 704 μm^2 for LG U, 4978 ± 826 μm^2 for AG U, 5494 ± 705 μm^2 for CG U, 2312 ± 601 μm^2 for LG CT, 2444 ± 1194 μm^2 for AG CT, 2515± 814 μm^2 for CG CT, 3545 ± 705 μm^2 for LG CTS, 4232 ± 959 μm^2 for AG CTS and 5082 ± 799 μm^2 for CG CTS. With

different glycemic conditions (figure 2.8A), mean value of cell area was significantly greater for chronic high glucose treatment in unloaded control (p-value < 0.0001) and CTS samples (p < 0.0001) whereas for acute hyperglycemic conditions cell area was observed to be higher than low glucose controls under unloaded and CTS however, statistical significance was not observed. Application of cyclic tensile resulted in similar mean cell area values for all glycemic conditions.

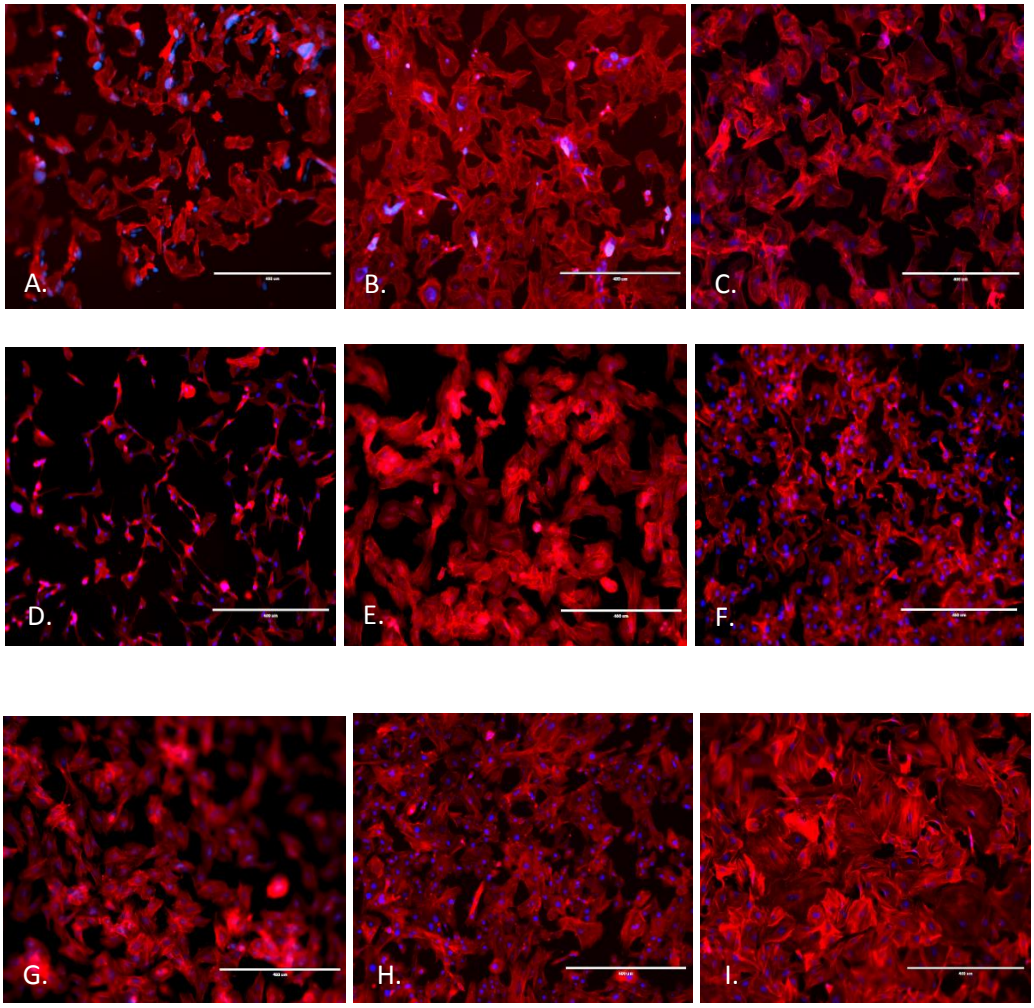

Figure 2.7: *Rhodamine-Phalloidin Images for Low Glucose (left column), Acute High Glucose (Center Column) and Chronic High glucose (Right Column) with Unloaded (A-C), Cyclic Tensile (D-F) and Cyclic Tensile Shear (G-I) at 100x magnification, Scale bar-400 µm.*

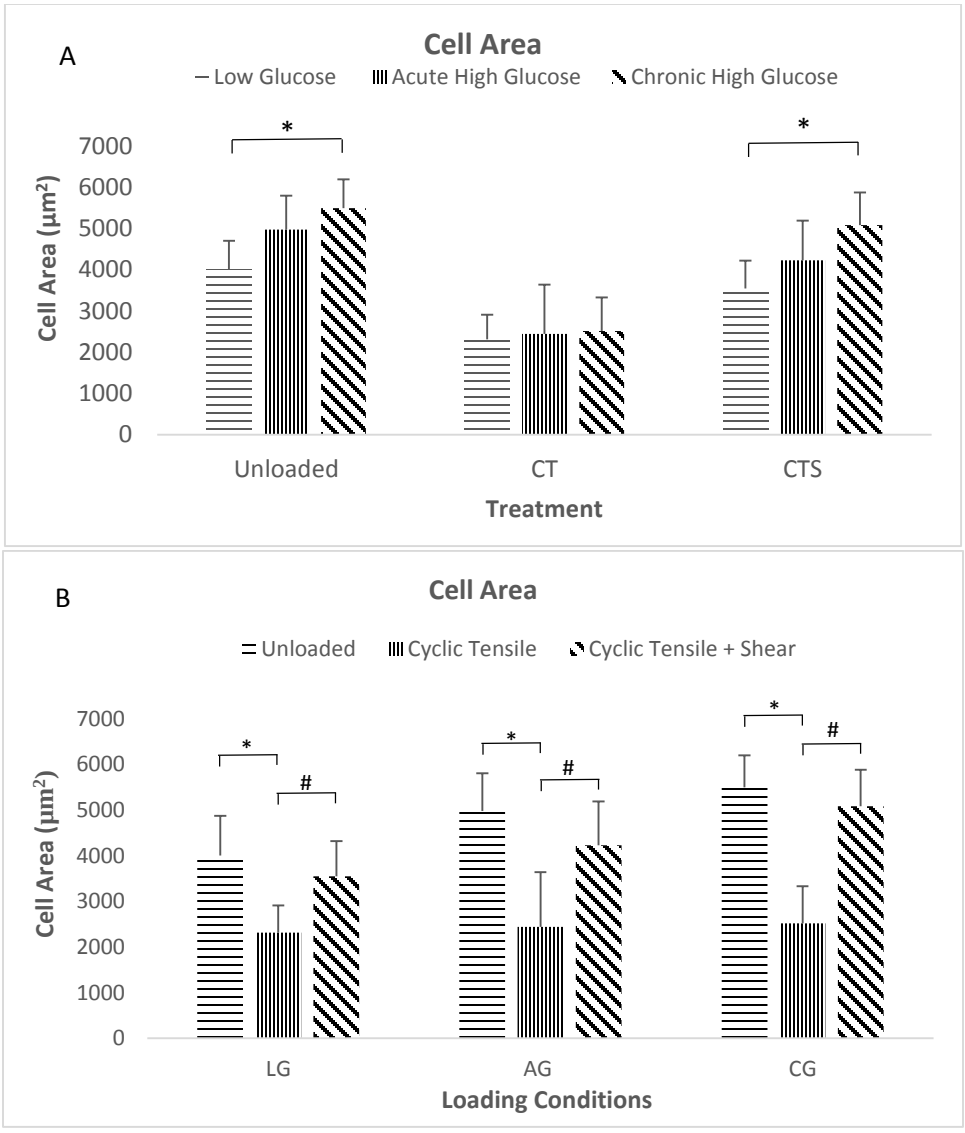

Figure 2.8: *Values represented as Mean ± SD (error bar) with n = 125 for each sample. A). '*' represents p-value < 0.05 when compared to low glucose controls within each simulation group. '#' represents p-value < 0.05 for chronic samples when compared to acute high glucose samples within each simulation group. B). '*' represents p-value < 0.05 when compared to unloaded simulation, '#' represents p-value < 0.05 for cyclic-tensile shear samples when compared to cyclic tensile simulation for each glycemic group. All comparison performed with One-way ANOVA & Tukey post-hoc analysis.*

With different loading conditions (figure 2.8B), application of cyclic tensile strain led to a significant decrease in cell area for all glucose treatments ($p < 0.0001$ for LG, AG and CG) as compared to respective unloaded controls. In addition, application of cyclic tensile shear led to an increase in cell area for all glucose treatments ($p < 0.0001$ for LG, AG and CG). However, differences in cell area for unloaded and CTS were non-significant for all glucose treatments. Data values for cell area are summarized in table 2.4.

Sample	Unloaded (U)	Cyclic Tensile (CT)	Cyclic Tensile + Shear (CTS)
Low glucose (LG)	4003 ± 704 μm^2	2312 ± 601 μm^2	3545 ± 705 μm^2
Acute high (AG)	4978 ± 826 μm^2	2444 ± 1194 μm^2	4232 ± 959 μm^2
Chronic high (CG)	5494 ± 705 μm^2	2515± 814 μm^2	5082 ± 799 μm^2

Table 2.4: *Data values for Cell area (represented as Mean ± SD μm^2), n=125*

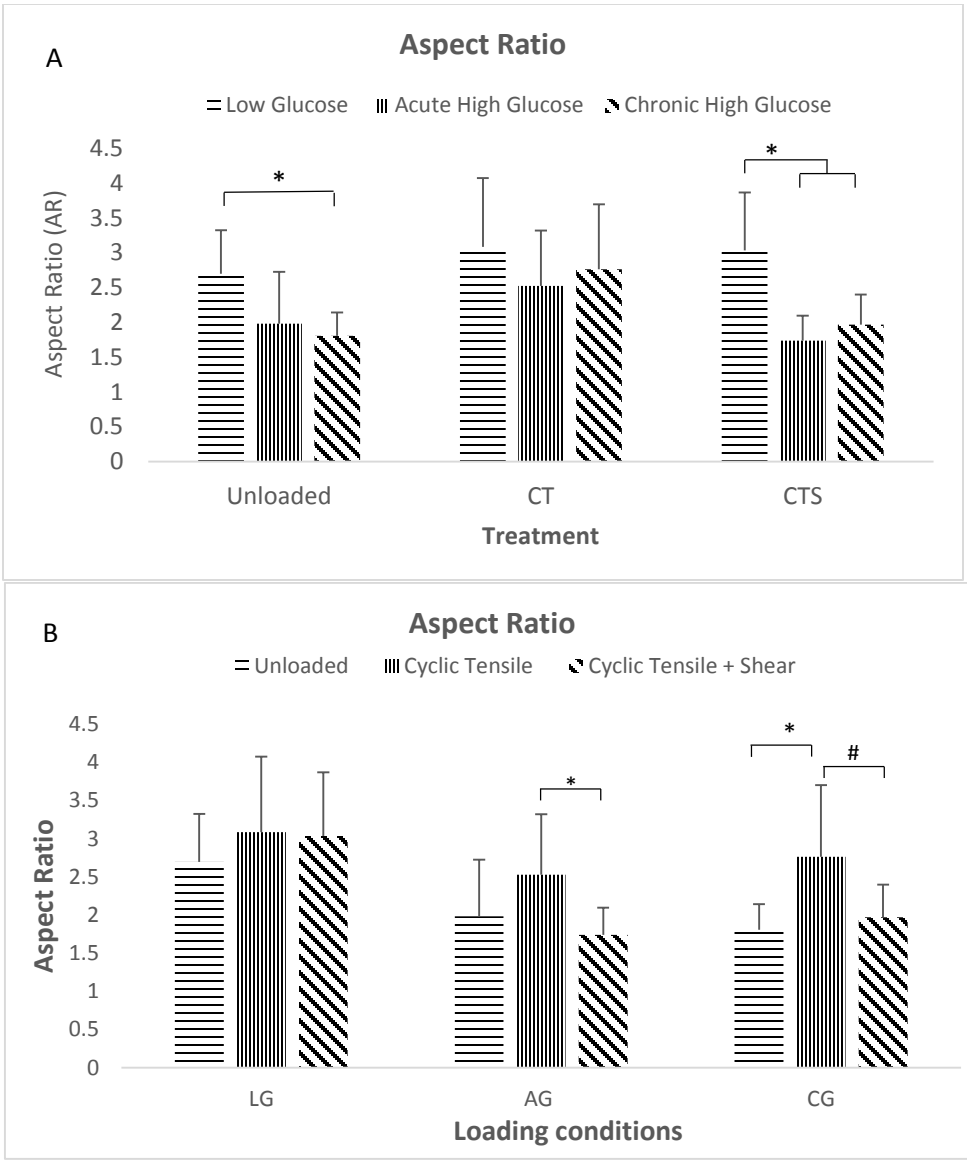

Figure 2.9: *Values represented as Mean ± SD (error bar) with n = 125 for each sample. A). '*' represents p-value < 0.05 when compared to low glucose controls within each simulation group. '#' represents p-value < 0.05 for chronic samples when compared to acute high glucose samples within each simulation group. B). '*' represents p-value < 0.05 when compared to unloaded simulation, '#' represents p-value < 0.05 for cyclic-tensile shear samples when compared to cyclic tensile simulation for each glycemic group. All comparison performed with One-way ANOVA & Tukey post-hoc analysis.*

Cell Aspect ratio (AR), which is a ratio of major axis length to minor axis length of a cell, was observed to be 2.69 ± 0.62 for LG U, 1.98 ± 0.74 for AG U, 1.81 ± 0.33 for CG U, 3.08 ± 0.98 for LG CT, 2.52 ± 0.79 for AG CT, 2.76 ± 0.93 for CG CT, 3.03 ± 0.83 for LG CTS, 1.73 ±

0.36 for AG CTS and 1.96 ± 0.42 for CG CTS. For different glycemic conditions (figure 2.9A), mean aspect ratio for CT samples was observed to be nearly the same. Chronic hyperglycemic samples demonstrated a significantly lower aspect ratio under CTS loading conditions (p-value < 0.0001) and unloaded control (p-value < 0.0001) when compared to low glucose control. Acute hyperglycemia demonstrated a reduced mean aspect ratio across all treatments in comparison to low glucose controls, albeit statistical significance was only achieved in case of CTS treatment (p-value = 0.0001). With different loading conditions (figure 2.9B), application of cyclic tensile strain led to an increase in aspect ratio across all glucose treatments although significant increase was only observed in case of chronic high glucose (p < 0.0001) in comparison to respective unloaded controls. Application of cyclic tensile-shear led to a significant increase only in case of acute and chronic high glucose in comparison to cyclic tensile conditions (p < 0.0001 for both AG and CG). However, in comparison to unloaded controls, no significant changes were observed for all glucose treatments. Data values for cell aspect ratio are summarized in table 2.5.

Sample	Unloaded (U)	Cyclic Tensile (CT)	Cyclic Tensile + Shear (CTS)
Low glucose (LG)	2.69 ± 0.62	3.08 ± 0.98	3.03 ± 0.83
Acute high (AG)	1.98 ± 0.74	2.52 ± 0.79	1.73 ± 0.36
Chronic high (CG)	1.81 ± 0.33	2.76 ± 0.93	1.96 ± 0.42

Table 2.5: *Data values for Cell aspect ratio (represented as Mean ± SD), n=125*

Quantification of Protein Markers

Expression levels of contractile-state associated proteins were compared with western blotting. Markers evaluated in the current study included SM α-Actin, Calponin and SM 22α. Expression levels of these proteins were normalized to the expression of α-tubulin. SM α-actin expression levels (figure 2.10) were significantly less for acute hyperglycemic samples for CTS loading (p-value = 0.0001) and unloaded controls (p-value = 0.003). Similarly, chronic samples also had

reduced expression of SM α-actin under CTS (p-value = 0.0001) and unloaded controls however statistical significance for unloaded controls was not reached. Expression levels of actin did not differ between different glycemic groups.

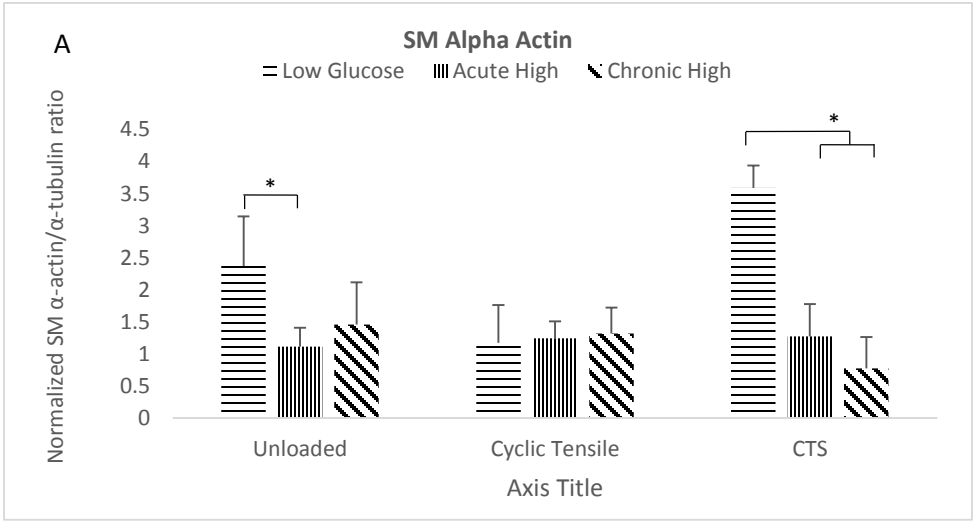

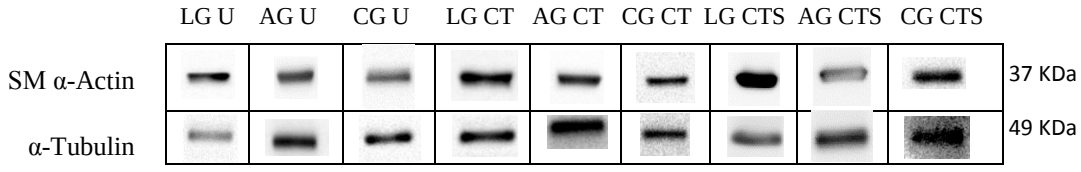

Figure 2.10: *Values represented as Mean ± SD (error bar) with n = 6 for each sample. A). '*' represents p-value < 0.05 when compared to low glucose controls within each simulation group. '#' represents p-value < 0.05 for chronic samples when compared to acute high glucose samples within each simulation group. B). '*' represents p-value < 0.05 when compared to unloaded simulation, '#' represents p-value < 0.05 for cyclic-tensile shear samples when compared to cyclic tensile simulation for each glycemic group. All comparison performed with One-way ANOVA & Tukey post-hoc analysis. U = Unloaded, CT = Cyclic Tensile, CTS = Cyclic Tensile shear; LG = low glucose, AG = acute high glucose, CG = chronic high glucose*

With different loading conditions, application of cyclic tensile shear results in a significant decrease in alpha-actin for chronic high glucose ($p = 0.0077$) only as compared to unloaded condition. In contrast, application of cyclic tensile-shear led to an increase in actin expression as compared to unloaded conditions in case low glucose however, difference was non-significant ($p = 0.298$).

Expression levels of calponin (figure 2.11A) were in agreement with low SM α-actin levels as chronic and acute samples exhibited reduced expression across unloaded and CTS in comparison to low glucose controls however, significant difference was only observed for chronic samples (p-value = 0.0002 for U, p-value < 0.0001 for CTS). In addition, calponin expression was observed to be significantly reduced for chronic samples even in comparison to acute hyperglycemia (p-value = 0.0208 for U, p-value = 0.0001 for CTS). For cyclic tensile only, there was marked reduction in calponin expression for chronic sample when compared to both low glucose controls (p-value < 0.0001) and acute high glucose (p-value = 0.0084). Between different loading conditions (figure 2.11B), there was a decrease in calponin expression between unloaded and cyclic tensile shear samples for low glucose and chronic high treatments however, significant differences were not observed.

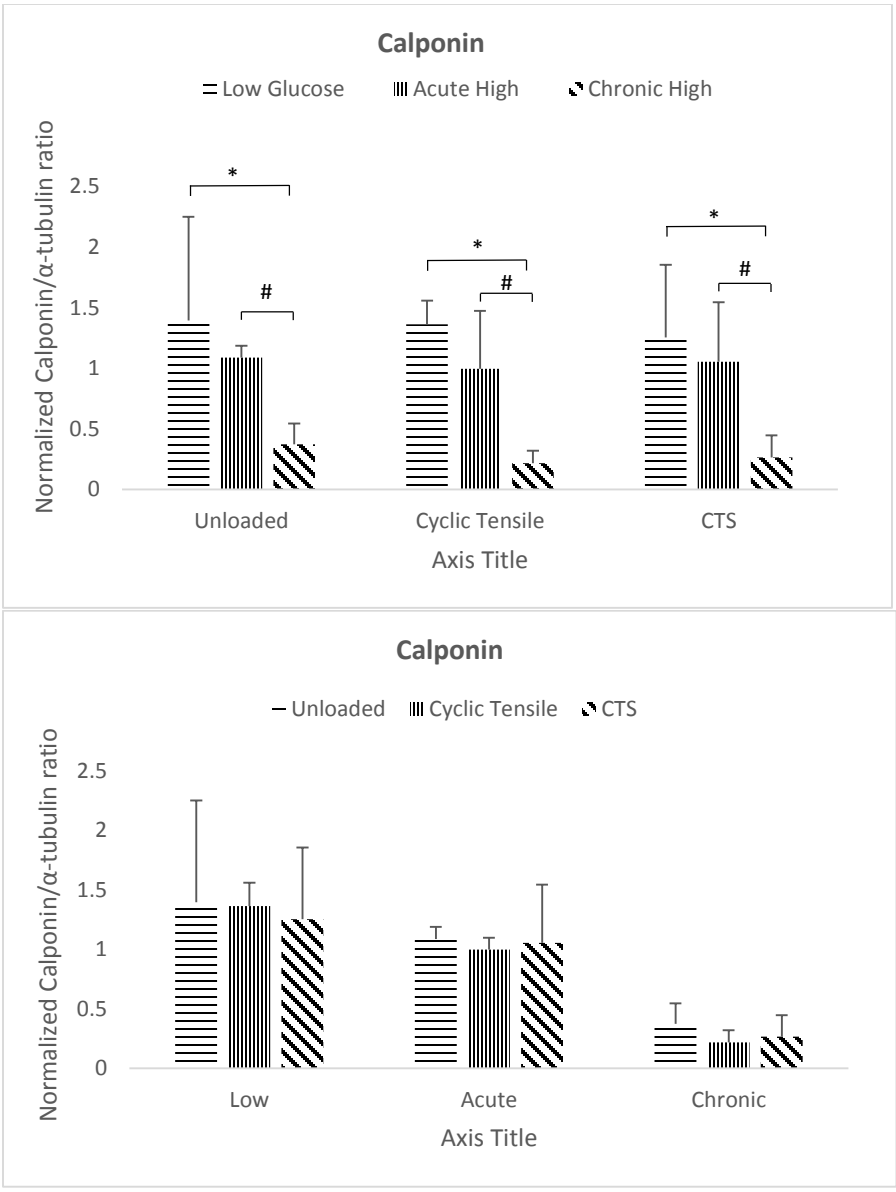

Figure 2.11: *Values represented as Mean ± SD (error bar) with n = 6 for each sample. A). '*' represents p-value < 0.05 when compared to low glucose controls within each simulation group. '#' represents p-value < 0.05 for chronic samples when compared to acute high glucose samples within each simulation group. B). '*' represents p-value < 0.05 when compared to unloaded simulation, '#' represents p-value < 0.05 for cyclic-tensile shear samples when compared to cyclic tensile simulation for each glycemic group. All comparison performed with One-way ANOVA & Tukey post-hoc analysis. U = Unloaded, CT = Cyclic Tensile, CTS = Cyclic Tensile shear; LG = low glucose, AG = acute high glucose, CG = chronic high glucose.*

SM22α expression levels (figure 2.12A) remained nearly the same under all glycemic conditions for unloaded controls. However, application of mechanical forces led to a significantly reduced expression of SM22α under both acute (p-value = 0.0259 for CT, p-value =0.0002 for CTS) and chronic hyperglycemia (p-value = 0.0210 for CT, p-value = 0.0008 for CTS) in comparison to low glucose controls.

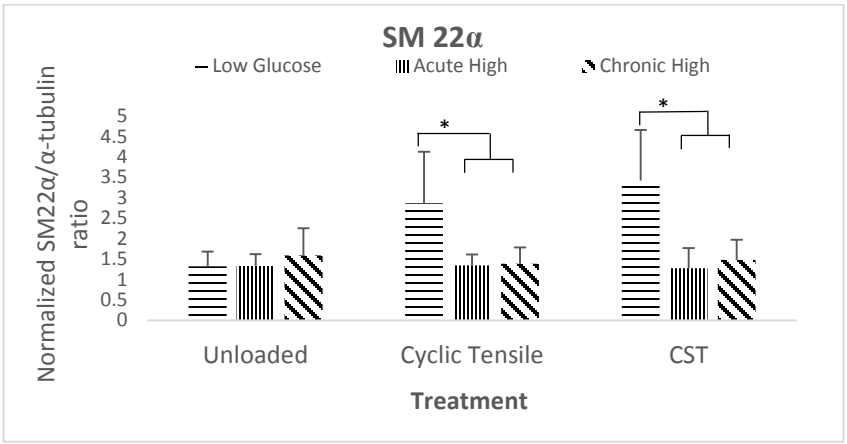

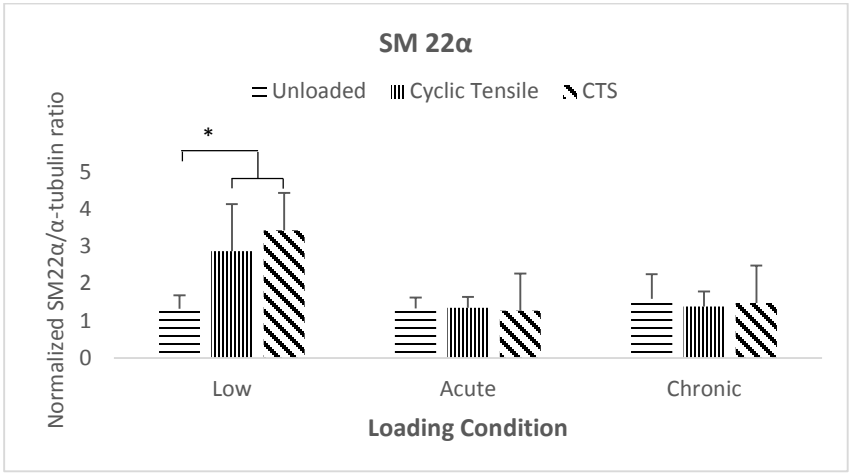

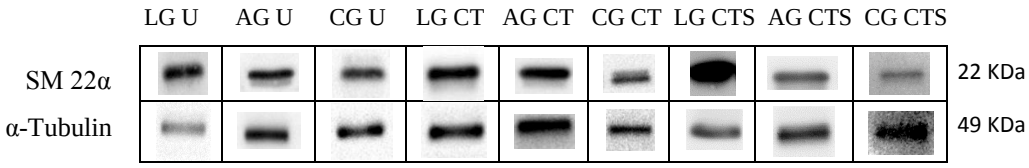

Figure 2.12: *Values represented as Mean ± SD (error bar) with n = 6 for each sample. A). '*' represents p-value < 0.05 when compared to low glucose controls within each simulation group. '#' represents p-value < 0.05 for chronic samples when compared to acute high glucose samples within each simulation group. B). '*' represents p-value < 0.05 when compared to unloaded simulation, '#' represents p-value < 0.05 for cyclic-tensile shear samples when compared to cyclic tensile simulation for each glycemic group. All comparison performed with One-way ANOVA & Tukey post-hoc analysis. U = Unloaded, CT = Cyclic Tensile, CTS = Cyclic Tensile shear; LG = low glucose, AG = acute high glucose, CG = chronic high glucose.*

With different glycemic conditions (figure 2.12B), application of cyclic tensile and cyclic tensile-shear resulted a significant increase in expression of SM22 alpha ($p = 0.014$ for CT, $p = 0.0002$ for CTS) in comparison to unloaded controls. However, differences were not significant for acute and chronic high glucose treatments for all loading conditions.

2.4 Discussion

Hyperglycemia is a clinical metabolic complication associated with diabetic patients and poor glycemic control has been associated with poor outcomes of percutaneous coronary intervention, for both angioplasty and stents [138-140, 185-187]. Effects of mechanical forces under hyperglycemic conditions have not been explored and thus, using a vascular simulator capable of concomitant strain and shear application [188], we explored the influence of hyperglycemia on phenotypic modulation of rat aortic SMCs under mechanically loaded conditions.

Clinically, VSMCs experience mechanical forces such as cyclic strain due to arterial distension and compression in addition to shear forces from blood flow, which come into play after denudation of the endothelium or migration of VSMCs to the intima. Using 3D-reconstruction and mesh approach, Garcia and collaborators [64] and LaDisa and collaborators [176] demonstrated neointimal growth to be negatively correlated with shear stress in the intra-stent regions in humans and animal models respectively. Phenotypic modulation of vascular smooth muscle cells is one of the early cellular response to the barotrauma from a PCI procedure resulting in a migratory and proliferative synthetic phenotype which contributes to neointimal hyperplasia [166]. Phenotypic modulation of VSMCs from a contractile to a synthetic state is associated with increased proliferation, increased cellular hypertrophy, decreased expression contractile-state associated proteins including SM-α actin, SM22-α, and calponin [168].

In the current study, we investigated the effects of different glycemic conditions on passage 2-5 rat aortic smooth muscle cell phenotype when subjected to different mechanical loading conditions.

Glycemic conditions investigated were low glucose or LG (5.5 mM glucose during seeding and mechanical loading), acute high glucose or AG (25 mM glucose during seeding and mechanical loading) and chronic high glucose or CG (cells acclimated with 25 mM glucose for 3-4 weeks before testing and during mechanical loading). Mechanical loading conditions included unloaded or U (static), cyclic tensile or CT (0-7% cyclic stretch at 1Hz for 24 hours) and cyclic tensile shear or CTS (0-7% cyclic stretch at 1Hz and ~ 0.30 dynes.cm^{-2} shear stress for 24 hours). Characterization of SMC phenotypic modulation was performed by evaluating changes in cellular proliferation, percentage of apoptotic cells, cellular hypertrophy estimated by comparing average of cell area and aspect ratio of imaged cells across all samples and comparing the expression levels of contractile-state associated markers.

Within the smooth muscle cell continuum, synthetic cells have been shown to exhibit greater rates of proliferation as compared to contractile phenotype. Application of physiological levels of strain have been reported to cause cell cycle arrest thereby inhibiting VSMC proliferation [189]. Results from our study are in agreement with previous work since application of cyclic strain led to an overall decrease in cellular proliferation as compared to unloaded control whereas concomitant application of shear and strain resulted in an increased proliferative response in comparison to cyclic strain [188]. In the current study, exposure of hyperglycemic samples to concomitant shear and strain led to a significant increase in proliferation when compared to low glucose samples ($p < 0.0001$ for acute or AG; $p < 0.0001$ for chronic or CG). These results indicate that hyperglycemia is contributive to VSMC proliferation. Previous studies have demonstrated a proliferative response exhibited by VSMCs under high glucose conditions and cell-proliferation results for the unloaded controls (U) from our study are in accordance with them ($p < 0.0001$ for AG; $p < 0.0001$ for CG) [158]. However, to the best of our knowledge, increased proliferation under hyperglycemia in response to concomitant shear and strain has not been reported before. Although, mechanisms involved in increasing proliferation under mechanically loaded conditions were not explored in our study, it is evident from current results that exposure of VSMCs to high glucose conditions and

mechanical forces led to an increased proliferation in comparison to low glucose conditions, which may be indicative of increased phenotypic modulation in hyperglycemic groups. Wire injury in streptozotocin-induced diabetic mice has been shown to cause an increased neointimal hyperplasia attributed to hyperglycemia-mediated SMC growth and proliferation [181]. Further, in vitro studies with arterial and venous smooth muscle cells from diabetic patients have also demonstrated an increased proliferation of VSMCs, as compared to non-diabetic controls [190, 191]. Consistent with these studies, results from our study also indicate a similar response, of increased proliferation, exhibited by cells subjected to CTS conditions under hyperglycemia thus supporting the relevance of this dynamic disease model designed to subject VSMCs, cultured in different glycemic conditions, to clinically relevant mechanical forces.

In addition to proliferation, VSMC apoptosis also plays a critical role in neo-intimal formation after vessel injury. Studies have reported a rapid apoptosis after angioplasty with up to 70% of VSMCs becoming apoptotic within 90 minutes [192]. In mouse flow cessation studies, VSMC apoptosis was shown to cause migration, proliferation and extracellular matrix secretion of neighboring VSMCs and led to a thicker neo-intima despite significant apoptosis. These results were shown to be mediated by IL-6 release which has been shown to cause VSMC proliferation and promote migration [193]. Similarly, in rat models of balloon-injury, medial cells have been shown to undergo apoptosis from 30 min to 4 hours post-dilation [194]. Although the exact contribution of apoptosis to the development of neo-intimal hyperplasia is unclear, it still represents one of the earliest response of the resident cells. Thus, an apoptotic response can be correlated with increased synthetic-state characteristics since higher proliferation and apoptosis may also represent a higher cell turnover rate associated with dedifferentiation [184]. Results from the current study illustrate an increase in percentage of apoptotic cells under both acute and chronic hyperglycemia across all mechanical loading conditions in comparison to low glucose controls, however statistical significance for acute CTS was not observed ($p = 0.0842$). Further, apoptosis was reported to be higher for CTS loading in all glycemic conditions in comparison to CT. These results indicate that

hyperglycemia and mechanical forces are contributive to apoptosis and this response is more pronounced with the application of low shear stress. Low shear stress led to an increased overall apoptotic capacity even in low glucose samples, although significantly less than chronic samples ($p < 0.0001$). In vitro application of low shear stress has been shown to increase Rac1-Rho phosphorylation in VSMCs [195]. This, in part, may explain the role of low shear in mediating a pro-apoptotic behavior [196]. Another mechanism that may contribute to increased apoptosis is hyperglycemia-mediated reactive oxygen species generation which has been implicated as a contributor to VSMC apoptosis via upregulation of hydrogen peroxide in other studies [197].

Cellular hypertrophy, indicative of increased cell size, has been employed as an estimate of phenotypic modulation since synthetic state cells are generally more rhomboid/epithelioid-shaped as compared to spindle-like contractile cells. In addition, an organized F-actin structure, which is involved in maintaining contractile functions, is associated with the contractile-state phenotype whereas a diffuse loose F-actin structure is exhibited by synthetic cells [198]. Estimation of cellular hypertrophy by measuring average cell area of imaged cells revealed a greater cell area under both acute and chronic hyperglycemic conditions compared to low glucose samples in unloaded controls as well as in CTS simulations, however the differences for were significant only for CG U($p< 0.0001$) and CG CTS ($p < 0.0001$) compared to LG U and LG CTS respectively. Further, application of cyclic strain led to an overall decrease in cell area across all samples thus demonstrating the influence of concomitant shear and strain on cell morphology. In agreement with the results of increased cell area, mean cell aspect ratio was also observed to be lower for both AG U and CG U ($p<0.0001$ for CG U only, non-significant for AG U) compared to LG U with lower aspect ratio for AG CTS and CG CTS loading ($p<0.0001$ for AG, $p < 0.0001$ for CG) in comparison to LG CTS. These results indicate an increased cellular hypertrophy of VSMCs under both short and long term hyperglycemic conditions compared to low glucose CTS controls. Results of cellular hypertrophy from previous studies have demonstrated similar effects, with application of strain and shear resulting in an overall decrease in aspect ratio, thus subordinating our CTS results [188]. VSMCs

from diabetic patients have been reported to attain an altered and rhomboid-shape cell shape with a loss of the typical 'hill-valley' morphology as compared to non-diabetic controls [190, 191] and these morphological changes have been consistent in neo-intimal lesions [199]. These studies are in agreement with our observations where high glucose conditions resulted in a more rounded morphology leading to a lower cell aspect ratio thus supporting the relevance of our dynamic disease model.

Expression levels of contractile-state associated proteins is one of the most important distinguishing markers of SMC phenotype. As mentioned before, contractile state of VSMCs is characterized by greater expression of contractile-apparatus proteins and in the current study we evaluated the expression levels of SM α-actin, SM22 α and calponin normalized to α-tubulin. With cyclic strain, nearly the same SM α-actin expression levels were observed for all three glycemic groups. Interestingly with cyclic strain, calponin and SM22α levels were significantly reduced for chronic samples ($p < 0.0001$ for calponin, $p = 0.0210$ for SM22α) whereas significance was only observed for SM22α in case of acute conditions ($p = 0.0259$), in comparison to low glucose CT. Further, chronic glucose (CG) led to a significantly decreased expression of SM α-actin, SM22 alpha and calponin under CTS condition ($p < 0.0001$, $p = 0.0008$, $p < 0.0001$ respectively) in comparison to LG CTS. In addition, CG CTS led to a lower expression of actin and calponin, but not SM22α in comparison to AG CTS, however significant reduction was only observed in calponin expression ($p < 0.0001$). Thus, both acute and chronic hyperglycemic samples exhibited a more synthetic phenotype in comparison to low glucose controls under CTS, with chronic hyperglycemia resulting in a relatively greater synthetic response as estimated from significantly lower levels of SM α-actin and calponin expression in chronic CTS (CG CTS). Protein expression results from previous studies have demonstrated a reduction in SM α-actin and calponin in VSMCs isolated from rat models of type 1 diabetes [200, 201] and type 2 diabetes [202] respectively. These results are in agreement with our observation of reduced expression levels of all three markers (SM α-actin, SM22 α and calponin) in chronic hyperglycemic samples subjected to clinically relevant mechanical forces in

our dynamic disease model. Thus, concomitant application of shear and strain to vascular smooth muscle cells subjected to chronic hyperglycemia led to an overall increase the synthetic activity of cells as evident from increased proliferation and apoptosis, cellular hypertrophy and decreased expression of contractile-state associated markers thereby providing conclusive results to prove our proposed hypothesis. In future, this model could be used to evaluate novel drugs aimed at reducing restenosis in diabetes or compare the efficacy of existing drugs.

2.5 Conclusion

In the current study we assessed the relative differences in phenotypic modulation of vascular smooth muscle cells due to mechanical loading and hyperglycemia by comparing cellular proliferation, apoptosis, hypertrophy and expression of contractile-state markers. Results from the study indicate a direct contribution of hyperglycemia to phenotypic modulation of SMCs in acute and chronic samples. With cyclic strain only conditions, nearly the same response was observed in acute and chronic samples with slight evidence of de-differentiation observed as compared to low glucose controls & no significant difference between acute and chronic samples. However, application of low shear with cyclic strain (CTS) led to a significant difference in the response of all groups with acute (AG CTS) and chronic (CG CTS) samples eliciting a relatively greater phenotypic modulation in comparison to respective low glucose control (LG CTS). Thus, these results indicate that only low shear stress may be contributive to glycaemia-mediated phenotypic modulation. In addition, although differences between acute and chronic samples were not similar for all assays, chronic samples did express higher rates of apoptosis consistently. Importantly, we did not explore the potential mechanisms involved in manifestation of these effects and thus exploration of the mechanisms will require further research. In conclusion, increased phenotypic modulation was observed for hyperglycemic VSMCs subjected to low shear stress and cyclic strain (CTS) with increased apoptosis for chronic hyperglycemia across all loading conditions. Similarity

of VSMC response between our model and diabetes-associated phenotypic changes support the relevance of our model. This model may serve a useful role in exploring the effects of diabetes-related metabolic complications at a cellular levels in conjunction with precisely controlled hemodynamics.

Project Recommendations:

1. Application of this model can be extended to response evaluation of other metabolic-complications and mechanical forces. Clinically, insulin treated diabetic patients are at increased risk of developing MACE (Major adverse cardiac events) and TVF even with use of second generation drug eluting stents. Thus, this model can be utilized in evaluating the response to insulin mediated VSMC response to low shear forces. In addition to exploring phenotypic modulation, this models can be applied to inflammatory cells in applications such as increased inflammatory markers in the circulating media or macrophage-conditioned media and their contribution to the VSMC response.

2. Using the same bioreactor system, efficacy of different anti-restenotic drugs can be compared in reference to altered hemodynamics such as paclitaxel, sirolimus or exogenous administration of nitric oxide on VSMC phenotypic modulation in altered hemodynamics and diabetes-related metabolic environment. However, drug administration approach should closely mimic the kinetics of the drug in vivo.

3. In order to increase the clinical relevance of the current model, lid designs can be exploited to reduce channel height which would enable the application of physiological and high shear stresses and thus compare responses in normal and diseased milieu.

4. In the current study, type 1 collagen was used as the seeding matrix for VSMCs. Mechanotransduction is also influenced by the type of ECM and this model can be used to compare cellular response of different ECM matrices and can also be extended to evaluate the response on modified matrices such as glycated ECM molecules to improve our current understanding of diabetes.

References:

1. Armstrong, E.J., J.C. Rutledge, and J.H. Rogers, *Coronary Artery Revascularization in Patients With Diabetes Mellitus.* Circulation, 2013. **128**(15): p. 1675-1685.
2. J. Gordon Betts, T.J.C., et al., *Anatomy and Physiology* 2013, Open Stax College.
3. Kwak, B.R., et al., *Biomechanical factors in atherosclerosis: mechanisms and clinical implications.* Eur Heart J, 2014. **35**(43): p. 3013-20.
4. Conway, D.E., S.G. Eskin, and L.V. McIntire, *Chapter II.1.6 - Effects of Mechanical Forces on Cells and Tissues (The Liquid–Cell Interface)*, in *Biomaterials Science (Third Edition)*, B.D.R.S.H.J.S.E. Lemons, Editor 2013, Academic Press. p. 474-487.
5. Dobrin, P.B., F.N. Littooy, and E.D. Endean, *Mechanical factors predisposing to intimal hyperplasia and medial thickening in autogenous vein grafts.* Surgery, 1989. **105**(3): p. 393-400.
6. Goldsmith, H.L. and V.T. Turitto, *Rheological aspects of thrombosis and haemostasis: basic principles and applications. ICTH-Report--Subcommittee on Rheology of the International Committee on Thrombosis and Haemostasis.* Thromb Haemost, 1986. **55**(3): p. 415-35.
7. Matsumoto, T. and K. Hayashi, *Mechanical and dimensional adaptation of rat aorta to hypertension.* J Biomech Eng, 1994. **116**(3): p. 278-83.
8. Humphrey, J.D., *Cardiovascular Solid Mechanics*2002: Springer-Verlag New York.
9. Hayashi, K. and T. Naiki, *Adaptation and remodeling of vascular wall; biomechanical response to hypertension.* J Mech Behav Biomed Mater, 2009. **2**(1): p. 3-19.
10. Dewey, C.F., Jr., et al., *The dynamic response of vascular endothelial cells to fluid shear stress.* J Biomech Eng, 1981. **103**(3): p. 177-85.
11. Krueger, J.W., D.F. Young, and N.R. Cholvin, *An in vitro study of flow response by cells.* Journal of Biomechanics, 1971. **4**(1): p. 31-36.
12. Buga, G.M., et al., *Shear stress-induced release of nitric oxide from endothelial cells grown on beads.* Hypertension, 1991. **17**(2): p. 187-93.
13. Korenaga, R., et al., *Laminar flow stimulates ATP- and shear stress-dependent nitric oxide production in cultured bovine endothelial cells.* Biochem Biophys Res Commun, 1994. **198**(1): p. 213-9.
14. Ohno, M., et al., *Shear stress elevates endothelial cGMP. Role of a potassium channel and G protein coupling.* Circulation, 1993. **88**(1): p. 193-7.
15. Frangos, J.A., et al., *Flow effects on prostacyclin production by cultured human endothelial cells.* Science, 1985. **227**(4693): p. 1477-9.
16. Sharefkin, J.B., et al., *Fluid flow decreases preproendothelin mRNA levels and suppresses endothelin-1 peptide release in cultured human endothelial cells.* J Vasc Surg, 1991. **14**(1): p. 1-9.
17. Rieder, M.J., et al., *Suppression of angiotensin-converting enzyme expression and activity by shear stress.* Circ Res, 1997. **80**(3): p. 312-9.
18. Takada, Y., et al., *Fluid shear stress increases the expression of thrombomodulin by cultured human endothelial cells.* Biochem Biophys Res Commun, 1994. **205**(2): p. 1345-52.
19. Yamamoto, K. and J. Ando, *Molecular Mechanisms Underlying Mechanosensing in Vascular Biology*, in *Mechanosensing Biology*, M. Noda, Editor 2011, Springer Japan. p. 21-37.

20. Diamond, S.L., S.G. Eskin, and L.V. McIntire, *Fluid flow stimulates tissue plasminogen activator secretion by cultured human endothelial cells.* Science, 1989. **243**(4897): p. 1483-5.
21. Haga, J.H., Y.S. Li, and S. Chien, *Molecular basis of the effects of mechanical stretch on vascular smooth muscle cells.* J Biomech, 2007. **40**(5): p. 947-60.
22. Hu, Y., et al., *Activation of PDGF receptor alpha in vascular smooth muscle cells by mechanical stress.* Faseb J, 1998. **12**(12): p. 1135-42.
23. Iwasaki, H., et al., *Mechanical stretch stimulates growth of vascular smooth muscle cells via epidermal growth factor receptor.* Am J Physiol Heart Circ Physiol, 2000. **278**(2): p. H521-9.
24. Hansson, G.K., *Inflammation, atherosclerosis, and coronary artery disease.* N Engl J Med, 2005. **352**(16): p. 1685-95.
25. Siracuse, J. and E. Chaikof, *The Pathogenesis of Diabetic Atherosclerosis*, in *Diabetes and Peripheral Vascular Disease*, G.V. Shrikhande and J.F. McKinsey, Editors. 2012, Humana Press. p. 13-26.
26. Gu, L., et al., *Absence of monocyte chemoattractant protein-1 reduces atherosclerosis in low density lipoprotein receptor-deficient mice.* Mol Cell, 1998. **2**(2): p. 275-81.
27. Rudijanto, A., *The role of vascular smooth muscle cells on the pathogenesis of atherosclerosis.* Acta Med Indones, 2007. **39**(2): p. 86-93.
28. Malek, A.M., S.L. Alper, and S. Izumo, *Hemodynamic shear stress and its role in atherosclerosis.* Jama, 1999. **282**(21): p. 2035-42.
29. Libby, P., P.M. Ridker, and G.K. Hansson, *Progress and challenges in translating the biology of atherosclerosis.* Nature, 2011. **473**(7347): p. 317-325.
30. Tabas, I., K.J. Williams, and J. Boren, *Subendothelial lipoprotein retention as the initiating process in atherosclerosis: update and therapeutic implications.* Circulation, 2007. **116**(16): p. 1832-44.
31. Cybulsky, M.I. and M.A. Gimbrone, Jr., *Endothelial expression of a mononuclear leukocyte adhesion molecule during atherogenesis.* Science, 1991. **251**(4995): p. 788-91.
32. Palombo, D., et al., *Matrix metalloproteinases. Their role in degenerative chronic diseases of abdominal aorta.* J Cardiovasc Surg, 1999. **40**(2): p. 257-60.
33. Gawaz, M., et al., *Platelets induce alterations of chemotactic and adhesive properties of endothelial cells mediated through an interleukin-1-dependent mechanism. Implications for atherogenesis.* Atherosclerosis, 2000. **148**(1): p. 75-85.
34. Mamputu, J.C., A.C. Desfaits, and G. Renier, *Lipoprotein lipase enhances human monocyte adhesion to aortic endothelial cells.* J Lipid Res, 1997. **38**(9): p. 1722-9.
35. Mamputu, J.C., L. Levesque, and G. Renier, *Proliferative effect of lipoprotein lipase on human vascular smooth muscle cells.* Arterioscler Thromb Vasc Biol, 2000. **20**(10): p. 2212-9.
36. Shanahan, C.M. and P.L. Weissberg, *Smooth muscle cell heterogeneity: patterns of gene expression in vascular smooth muscle cells in vitro and in vivo.* Arterioscler Thromb Vasc Biol, 1998. **18**(3): p. 333-8.
37. Singh, R.B., et al., *Pathogenesis of atherosclerosis: A multifactorial process.* Experimental & Clinical Cardiology, 2002. **7**(1): p. 40-53.
38. Libby, P., *Molecular and cellular mechanisms of the thrombotic complications of atherosclerosis.* J Lipid Res, 2009. **50**(7): p. 18.
39. Singh, N.H. and P.A. Schneider, *Chapter 8 - Balloon Angioplasty Catheters*, in *Endovascular Surgery (Fourth Edition)*, W.S.M.S. Ahn, Editor 2011, W.B. Saunders: Philadelphia. p. 71-80.

40. van der Hoeven, B.L., et al., *Drug-eluting stents: results, promises and problems.* Int J Cardiol, 2005. **99**(1): p. 9-17.
41. Akin, I., et al., *Second- and third-generation drug-eluting coronary stents: progress and safety.* Herz, 2011. **36**(3): p. 190-6.
42. Jukema, J.W., et al., *Restenosis after PCI. Part 1: pathophysiology and risk factors.* Nat Rev Cardiol, 2011. **9**(1): p. 53-62.
43. Clowes, R.L.G.A.W., *Essentials of Restenosis For the Innterventional Cardiologist, Chapter 2: Epidemiology and Pathogenesis of Restenosis*. 1 ed. Contemporary Cardiology, ed. H.J. Duckers, Nabel, Elizabeth G., Serruys, Patrick W.2007: Humana Press. 458.
44. Fischman, D.L., et al., *A Randomized Comparison of Coronary-Stent Placement and Balloon Angioplasty in the Treatment of Coronary Artery Disease.* New England Journal of Medicine, 1994. **331**(8): p. 496-501.
45. Roiron, C., et al., *Drug eluting stents: an updated meta-analysis of randomised controlled trials.* Heart, 2006. **92**(5): p. 641-649.
46. Weintraub, W.S., *The pathophysiology and burden of restenosis.* Am J Cardiol, 2007. **100**(5A): p. 26.
47. Caixeta, A.M., et al., *[Analysis of elastic retraction in the 1st 15 minutes after coronary balloon angioplasty]*. Arq Bras Cardiol, 1996. **66**(1): p. 5-9.
48. Rodriguez, A.E., et al., *Time course and mechanism of early luminal diameter loss after percutaneous transluminal coronary angioplasty.* Am J Cardiol, 1995. **76**(16): p. 1131-4.
49. Rozenman, Y., et al., *Clinical and angiographic predictors of immediate recoil after successful coronary angioplasty and relation to late restenosis.* Am J Cardiol, 1993. **72**(14): p. 1020-5.
50. Rajagopal, V. and S.G. Rockson, *Coronary restenosis: a review of mechanisms and management.* Am J Med, 2003. **115**(7): p. 547-53.
51. Riessen, R., et al., *Distribution of hyaluronan during extracellular matrix remodeling in human restenotic arteries and balloon-injured rat carotid arteries.* Circulation, 1996. **93**(6): p. 1141-7.
52. Curcio, A., D. Torella, and C. Indolfi, *Mechanisms of smooth muscle cell proliferation and endothelial regeneration after vascular injury and stenting: approach to therapy.* Circ J, 2011. **75**(6): p. 1287-96.
53. Virmani, R., et al., *Drug eluting stents: are human and animal studies comparable?* Heart, 2003. **89**(2): p. 133-138.
54. Dzavik, V., *New frontiers and unresolved controversies in percutaneous coronary intervention.* Am J Cardiol, 2003. **91**(3A): p. 27A-33A.
55. Mitra, A.K. and D.K. Agrawal, *In stent restenosis: bane of the stent era.* Journal of Clinical Pathology, 2006. **59**(3): p. 232-239.
56. Rollins, B.J., *Chemokines.* Blood, 1997. **90**(3): p. 909-28.
57. Tanabe, K., et al., *Restenosis rates following bifurcation stenting with sirolimus-eluting stents for de novo narrowings.* The American Journal of Cardiology, 2004. **94**(1): p. 115-118.
58. Kim, M.S. and L.S. Dean, *In-Stent Restenosis.* Cardiovascular Therapeutics, 2011. **29**(3): p. 190-198.
59. Lee, M.S., et al., *Clinical presentation of patients with in-stent restenosis in the drug-eluting stent era.* J Invasive Cardiol, 2008. **20**(8): p. 401-3.
60. Farooq, V., B.D. Gogas, and P.W. Serruys, *Restenosis: Delineating the Numerous Causes of Drug-Eluting Stent Restenosis.* Circulation: Cardiovascular Interventions, 2011. **4**(2): p. 195-205.

61. Chieffo, A., et al., *Histopathology of clinical coronary restenosis in drug-eluting versus bare metal stents.* Am J Cardiol, 2009. **104**(12): p. 1660-7.
62. Meurice, T., et al., *Role of endothelial cells in restenosis after coronary angioplasty.* Fundam Clin Pharmacol, 1996. **10**(3): p. 234-42.
63. Liu, M.W., G.S. Roubin, and S.B. King, 3rd, *Restenosis after coronary angioplasty. Potential biologic determinants and role of intimal hyperplasia.* Circulation, 1989. **79**(6): p. 1374-87.
64. García, J., et al., *Study of the evolution of the shear stress on the restenosis after coronary angioplasty.* Journal of Biomechanics, 2006. **39**(5): p. 799-805.
65. Larsen, K., et al., *Capture of circulatory endothelial progenitor cells and accelerated re-endothelialization of a bio-engineered stent in human ex vivo shunt and rabbit denudation model.* Eur Heart J, 2012. **33**(1): p. 120-8.
66. Wentzel, J.J., et al., *Relationship Between Neointimal Thickness and Shear Stress After Wallstent Implantation in Human Coronary Arteries.* Circulation, 2001. **103**(13): p. 1740-1745.
67. Heise, M., et al., *Correlation of Intimal Hyperplasia Development and Shear Stress Distribution at the Distal End-side-anastomosis, in vitro Study Using Particle Image Velocimetry*. European Journal of Vascular and Endovascular Surgery, 2003. **26**(4): p. 357-366.
68. Koskinas, K.C., et al., *Role of Endothelial Shear Stress in Stent Restenosis and ThrombosisPathophysiologic Mechanisms and Implications for Clinical Translation.* Journal of the American College of Cardiology, 2012. **59**(15): p. 1337-1349.
69. Mehran, R., et al., *Angiographic patterns of in-stent restenosis: classification and implications for long-term outcome.* Circulation, 1999. **100**(18): p. 1872-8.
70. Kastrati, A., et al., *Restenosis after coronary placement of various stent types.* Am J Cardiol, 2001. **87**(1): p. 34-9.
71. Kobayashi, Y., et al., *Stented segment length as an independent predictor of restenosis.* J Am Coll Cardiol, 1999. **34**(3): p. 651-9.
72. Hilenski, L.L.G., Kathy K., *Vascular Medicine: A companion to braunwald's Heart disease, Chapter 3: Vascular smooth muscle cell*. Second ed, ed. J.A.B. Mark A.Creager, Joseph Loscalzo2013, Braunwald's Heart Disease: Elselvier.
73. Somlyo, A.P. and A.V. Somlyo, *Signal transduction and regulation in smooth muscle.* Nature, 1994. **372**(6503): p. 231-6.
74. Akata, T., *Cellular and molecular mechanisms regulating vascular tone. Part 1: basic mechanisms controlling cytosolic Ca2+ concentration and the Ca2+-dependent regulation of vascular tone.* J Anesth, 2007. **21**(2): p. 220-31.
75. Itoh, T., et al., *Effects of modulators of myosin light-chain kinase activity in single smooth muscle cells.* Nature, 1989. **338**(6211): p. 164-7.
76. Kamm, K.E. and J.T. Stull, *Regulation of smooth muscle contractile elements by second messengers.* Annu Rev Physiol, 1989. **51**: p. 299-313.
77. Beamish, J.A., et al., *Molecular Regulation of Contractile Smooth Muscle Cell Phenotype: Implications for Vascular Tissue Engineering.* Tissue Engineering. Part B, Reviews, 2010. **16**(5): p. 467-491.
78. Rensen, S.S.M., P. Doevendans, and G. van Eys, *Regulation and characteristics of vascular smooth muscle cell phenotypic diversity.* Netherlands Heart Journal, 2007. **15**(3): p. 100-108.

79. Owens, G.K., M.S. Kumar, and B.R. Wamhoff, *Molecular regulation of vascular smooth muscle cell differentiation in development and disease.* Physiol Rev, 2004. **84**(3): p. 767-801.
80. Ross, R., *Atherosclerosis--an inflammatory disease.* N Engl J Med, 1999. **340**(2): p. 115-26.
81. Chobanian, A.V., et al., *Seventh Report of the Joint National Committee on Prevention, Detection, Evaluation, and Treatment of High Blood Pressure*. Hypertension, 2003. **42**(6): p. 1206-1252.
82. Hermsmeyer, K., *Calcium channel function in hypertension.* J Hum Hypertens, 1993. **7**(2): p. 173-6.
83. Blacher, J., et al., *Influence of biochemical alterations on arterial stiffness in patients with end-stage renal disease.* Arterioscler Thromb Vasc Biol, 1998. **18**(4): p. 535-41.
84. Demer, L.L., *Effect of calcification on in vivo mechanical response of rabbit arteries to balloon dilation.* Circulation, 1991. **83**(6): p. 2083-93.
85. Demer, L. and Y. Tintut, *Chapter 106 - Vascular Calcification*, in *Muscle*, J.A.H.N. Olson, Editor 2012, Academic Press: Boston/Waltham. p. 1383-1389.
86. Boström, K., et al., *Bone morphogenetic protein expression in human atherosclerotic lesions.* Journal of Clinical Investigation, 1993. **91**(4): p. 1800-1809.
87. Shanahan, C.M., et al., *Medial localization of mineralization-regulating proteins in association with Monckeberg's sclerosis: evidence for smooth muscle cell-mediated vascular calcification.* Circulation, 1999. **100**(21): p. 2168-76.
88. Li, X., H.Y. Yang, and C.M. Giachelli, *BMP-2 promotes phosphate uptake, phenotypic modulation, and calcification of human vascular smooth muscle cells.* Atherosclerosis, 2008. **199**(2): p. 271-7.
89. Steitz, S.A., et al., *Smooth muscle cell phenotypic transition associated with calcification: upregulation of Cbfa1 and downregulation of smooth muscle lineage markers.* Circ Res, 2001. **89**(12): p. 1147-54.
90. Ailawadi, G., et al., *Smooth muscle phenotypic modulation is an early event in aortic aneurysms.* J Thorac Cardiovasc Surg, 2009. **138**(6): p. 1392-9.
91. Services, U.d.o.H.a.H., *National DIabetes Statisitcs report*, 2014, Center for Disease Control: Atlanta, GA USA.
92. Waller, B.F., et al., *Status of the coronary arteries at necropsy in diabetes mellitus with onset after age 30 years. Analysis of 229 diabetic patients with and without clinical evidence of coronary heart disease and comparison to 183 control subjects.* Am J Med, 1980. **69**(4): p. 498-506.
93. McGuire, D.K. and N. Marx, *Diabetes in Cardiovascular Disease: A Companion to Braunwald's Heart Disease: Expert Consult-Online*2015: Elsevier Health Sciences.
94. Bjornstad, P.R., Marian K., *Chapter 3: Type 1 Diaebtes Pathophysiology, Molecular mechanisms, Genetic Insights*. A companion to Braunwald's hear disease, ed. D.K.M. McGuire, Nicholas. Vol. 1. 2015.
95. Weber, M.B.N., K.M. Venkat, *Chapter 1 Defrinition and Epidemiology of type 2 diabetes; Diabetes in Cardiovascular disease*. A companion to braunwald's heart disease, ed. D.K.M. McGuire, Nicholas. Vol. 1. 2015: Elselvier.
96. Moreno, P.R., et al., *Coronary Composition and Macrophage Infiltration in Atherectomy Specimens From Patients With Diabetes Mellitus.* Circulation, 2000. **102**(18): p. 2180-2184.

97. Cipollone, F., et al., *The receptor RAGE as a progression factor amplifying arachidonate-dependent inflammatory and proteolytic response in human atherosclerotic plaques: role of glycemic control.* Circulation, 2003. **108**(9): p. 1070-7.
98. Jorge Plutzky, B.Z.a.J.D.B., *Chpater 12-Diabetes in cardiovascular disease*, ed. N.M. Darren K McGuire2015: Elselvier. 512.
99. Vinik, A.I., et al., *Platelet dysfunction in type 2 diabetes.* Diabetes Care, 2001. **24**(8): p. 1476-85.
100. Assert, R., et al., *Regulation of protein kinase C by short term hyperglycaemia in human platelets in vivo and in vitro.* Diabetologia, 2001. **44**(2): p. 188-95.
101. Lemkes, B.A., et al., *Hyperglycemia: a prothrombotic factor?* J Thromb Haemost, 2010. **8**(8): p. 1663-9.
102. Schaeffer, G., et al., *Alterations in platelet Ca2+ signalling in diabetic patients is due to increased formation of superoxide anions and reduced nitric oxide production.* Diabetologia, 1999. **42**(2): p. 167-76.
103. Hadi, H.A.R. and J.A. Suwaidi, *Endothelial dysfunction in diabetes mellitus.* Vascular Health and Risk Management, 2007. **3**(6): p. 853-876.
104. Moncada, S. and A. Higgs, *The L-arginine-nitric oxide pathway.* N Engl J Med, 1993. **329**(27): p. 2002-12.
105. Bouma, G., et al., *Increased Serum Levels of MRP-8/14 in Type 1 Diabetes Induce an Increased Expression of CD11b and an Enhanced Adhesion of Circulating Monocytes to Fibronectin.* Diabetes, 2004. **53**(8): p. 1979-1986.
106. Devaraj, S., et al., *Evidence of Increased Inflammation and Microcirculatory Abnormalities in Patients With Type 1 Diabetes and Their Role in Microvascular Complications.* Diabetes, 2007. **56**(11): p. 2790-2796.
107. Suganami, T., et al., *Role of the Toll-like Receptor 4/NF-κB Pathway in Saturated Fatty Acid–Induced Inflammatory Changes in the Interaction Between Adipocytes and Macrophages.* Arteriosclerosis, Thrombosis, and Vascular Biology, 2007. **27**(1): p. 84-91.
108. Bu, D.X., et al., *Activation of the ROCK1 branch of the transforming growth factor-beta pathway contributes to RAGE-dependent acceleration of atherosclerosis in diabetic ApoE-null mice.* Circ Res, 2010. **106**(6): p. 1040-51.
109. Christopher, J., et al., *Regulation of B2-kinin receptors by glucose in vascular smooth muscle cells*. Vol. 280. 2001. H1537-H1546.
110. Sun, J., et al., *Intermittent high glucose enhances proliferation of vascular smooth muscle cells by upregulating osteopontin.* Mol Cell Endocrinol, 2009. **313**(1-2): p. 64-9.
111. Li, S.L., et al., *Enhanced proatherogenic responses in macrophages and vascular smooth muscle cells derived from diabetic db/db mice.* Diabetes, 2006. **55**(9): p. 2611-9.
112. Reddy, M.A., et al., *Pro-inflammatory role of microrna-200 in vascular smooth muscle cells from diabetic mice.* Arterioscler Thromb Vasc Biol, 2012. **32**(3): p. 721-9.
113. Van Belle, E., et al., *Restenosis Rates in Diabetic Patients: A Comparison of Coronary Stenting and Balloon Angioplasty in Native Coronary Vessels.* Circulation, 1997. **96**(5): p. 1454-1460.
114. Carrozza, J.P., Jr., et al., *Restenosis after arterial injury caused by coronary stenting in patients with diabetes mellitus.* Ann Intern Med, 1993. **118**(5): p. 344-9.
115. Elezi, S., et al., *Diabetes mellitus and the clinical and angiographic outcome after coronary stent placement.* J Am Coll Cardiol, 1998. **32**(7): p. 1866-73.
116. Lau, K.W., et al., *Midterm angiographic outcome of single-vessel intracoronary stent placement in diabetic versus nondiabetic patients: a matched comparative study.* Am Heart J, 1998. **136**(1): p. 150-5.

117. Schofer, J., et al., *Influence of treatment modality on angiographic outcome after coronary stenting in diabetic patients: a controlled study.* J Am Coll Cardiol, 2000. **35**(6): p. 1554-9.
118. Abizaid, A., et al., *The influence of diabetes mellitus on acute and late clinical outcomes following coronary stent implantation.* J Am Coll Cardiol, 1998. **32**(3): p. 584-9.
119. Marso, S., et al. *The stenting in diabetics debate: insight from the large GUSTO IIb experience with extended follow-up*. in *Circulation*. 1998. LIPPINCOTT WILLIAMS & WILKINS 227 EAST WASHINGTON SQ, PHILADELPHIA, PA 19106 USA.
120. Kornowski, R., et al., *Increased restenosis in diabetes mellitus after coronary interventions is due to exaggerated intimal hyperplasia. A serial intravascular ultrasound study.* Circulation, 1997. **95**(6): p. 1366-9.
121. Moses, J.W., et al., *Sirolimus-eluting stents versus standard stents in patients with stenosis in a native coronary artery.* N Engl J Med, 2003. **349**(14): p. 1315-23.
122. Moussa, I., et al., *Impact of sirolimus-eluting stents on outcome in diabetic patients: a SIRIUS (SIRolImUS-coated Bx Velocity balloon-expandable stent in the treatment of patients with de novo coronary artery lesions) substudy.* Circulation, 2004. **109**(19): p. 2273-8.
123. Sabate, M., et al., *Randomized comparison of sirolimus-eluting stent versus standard stent for percutaneous coronary revascularization in diabetic patients: the diabetes and sirolimus-eluting stent (DIABETES) trial.* Circulation, 2005. **112**(14): p. 2175-83.
124. Spaulding, C., et al., *A Pooled Analysis of Data Comparing Sirolimus-Eluting Stents with Bare-Metal Stents.* New England Journal of Medicine, 2007. **356**(10): p. 989-997.
125. Caixeta, A., et al., *5-year clinical outcomes after sirolimus-eluting stent implantation insights from a patient-level pooled analysis of 4 randomized trials comparing sirolimus-eluting stents with bare-metal stents.* J Am Coll Cardiol, 2009. **54**(10): p. 894-902.
126. Raber, L., et al., *Five-year clinical and angiographic outcomes of a randomized comparison of sirolimus-eluting and paclitaxel-eluting stents: results of the Sirolimus-Eluting Versus Paclitaxel-Eluting Stents for Coronary Revascularization LATE trial.* Circulation, 2011. **123**(24): p. 2819-28.
127. Billinger, M., et al., *Long-term clinical and angiographic outcomes of diabetic patients after revascularization with early generation drug-eluting stents.* Am Heart J, 2012. **163**(5): p. 876-886.
128. Bangalore, S., et al., *Outcomes with various drug eluting or bare metal stents in patients with diabetes mellitus: mixed treatment comparison analysis of 22 844 patient years of follow-up from randomised trials*. Vol. 345. 2012.
129. Serruys, P.W., et al., *Percutaneous Coronary Intervention versus Coronary-Artery Bypass Grafting for Severe Coronary Artery Disease.* New England Journal of Medicine, 2009. **360**(10): p. 961-972.
130. Farkouh, M.E., et al., *Strategies for multivessel revascularization in patients with diabetes.* N Engl J Med, 2012. **367**(25): p. 2375-84.
131. Grube, E., et al., *The SPIRIT V diabetic study: a randomized clinical evaluation of the XIENCE V everolimus-eluting stent vs the TAXUS Liberte paclitaxel-eluting stent in diabetic patients with de novo coronary artery lesions.* Am Heart J, 2012. **163**(5): p. 867-875.
132. Stone, G.W., et al., *Differential Clinical Responses to Everolimus-Eluting and Paclitaxel-Eluting Coronary Stents in Patients With and Without Diabetes Mellitus.* Circulation, 2011.

133. Leon, M.B., et al., *A randomized comparison of the Endeavor zotarolimus-eluting stent versus the TAXUS paclitaxel-eluting stent in de novo native coronary lesions 12-month outcomes from the ENDEAVOR IV trial.* J Am Coll Cardiol, 2010. **55**(6): p. 543-54.
134. Jain, A.K., et al., *Twelve-month outcomes in patients with diabetes implanted with a zotarolimus-eluting stent: results from the E-Five Registry.* Heart, 2010. **96**(11): p. 848-53.
135. Briguori, C., et al., *Novel approaches for preventing or limiting events in diabetic patients (Naples-diabetes) trial: a randomized comparison of 3 drug-eluting stents in diabetic patients.* Circ Cardiovasc Interv, 2011. **4**(2): p. 121-9.
136. Silber, S., et al., *Clinical Outcome of Patients With and Without Diabetes Mellitus After Percutaneous Coronary Intervention With the Resolute Zotarolimus-Eluting Stent2-Year Results From the Prospectively Pooled Analysis of the International Global RESOLUTE Program.* JACC: Cardiovascular Interventions, 2013. **6**(4): p. 357-368.
137. Tian, F., et al., *Assessment of characteristics of neointimal hyperplasia after drug-eluting stent implantation in patients with diabetes mellitus: an optical coherence tomography analysis.* Cardiology, 2014. **128**(1): p. 34-40.
138. Hage, C., et al., *Glycaemic control and restenosis after percutaneous coronary interventions in patients with diabetes mellitus: a report from the Insulin Diabetes Angioplasty study.* Diab Vasc Dis Res, 2009. **6**(2): p. 71-9.
139. Corpus, R.A., et al., *Optimal glycemic control is associated with a lower rate of target vessel revascularization in treated type II diabetic patients undergoing elective percutaneous coronary intervention.* J Am Coll Cardiol, 2004. **43**(1): p. 8-14.
140. Lindsay, J., et al., *Preprocedure hyperglycemia is more strongly associated with restenosis in diabetic patients after percutaneous coronary intervention than is hemoglobin A1C.* Cardiovasc Revasc Med, 2007. **8**(1): p. 15-20.
141. Nusca, A., et al., *Prognostic role of preprocedural glucose levels on short- and long-term outcome in patients undergoing percutaneous coronary revascularization.* Catheter Cardiovasc Interv, 2012. **80**(3): p. 377-84.
142. Keating, F.K., B.E. Sobel, and D.J. Schneider, *Effects of increased concentrations of glucose on platelet reactivity in healthy subjects and in patients with and without diabetes mellitus.* Am J Cardiol, 2003. **92**(11): p. 1362-5.
143. Yamagishi, S., et al., *Advanced glycation end products (AGEs) and cardiovascular disease (CVD) in diabetes.* Cardiovasc Hematol Agents Med Chem, 2007. **5**(3): p. 236-40.
144. Undas, A., et al., *Hyperglycemia is associated with enhanced thrombin formation, platelet activation, and fibrin clot resistance to lysis in patients with acute coronary syndrome.* Diabetes Care, 2008. **31**(8): p. 1590-5.
145. Yngen, M., et al., *Acute hyperglycemia increases soluble P-selectin in male patients with mild diabetes mellitus.* Blood Coagul Fibrinolysis, 2001. **12**(2): p. 109-16.
146. Barlovic, D.P., A. Soro-Paavonen, and K.A. Jandeleit-Dahm, *RAGE biology, atherosclerosis and diabetes.* Clin Sci, 2011. **121**(2): p. 43-55.
147. Cefalu, W.T., et al., *Effect of combination glipizide GITS/metformin on fibrinolytic and metabolic parameters in poorly controlled type 2 diabetic subjects.* Diabetes Care, 2002. **25**(12): p. 2123-8.
148. Ii, M., et al., *Endothelial Progenitor Thrombospondin-1 Mediates Diabetes-Induced Delay in Reendothelialization Following Arterial Injury.* Circulation Research, 2006. **98**(5): p. 697-704.
149. Kuki, S., et al., *Hyperglycemia accelerated endothelial progenitor cell senescence via the activation of p38 mitogen-activated protein kinase.* Circ J, 2006. **70**(8): p. 1076-81.

150. Lindner, V. and M.A. Reidy, *Proliferation of smooth muscle cells after vascular injury is inhibited by an antibody against basic fibroblast growth factor.* Proceedings of the National Academy of Sciences of the United States of America, 1991. **88**(9): p. 3739-3743.
151. McClain, D.A., et al., *Glucose and glucosamine regulate growth factor gene expression in vascular smooth muscle cells.* Proc Natl Acad Sci U S A, 1992. **89**(17): p. 8150-4.
152. Mori, S., et al., *Hyperglycemia-induced alteration of vascular smooth muscle phenotype.* J Diabetes Complications, 2002. **16**(1): p. 65-8.
153. Srivastava, S., et al., *Contribution of aldose reductase to diabetic hyperproliferation of vascular smooth muscle cells.* Diabetes, 2006. **55**(4): p. 901-10.
154. Natarajan, R., et al., *Vascular smooth muscle cells exhibit increased growth in response to elevated glucose.* Biochem Biophys Res Commun, 1992. **187**(1): p. 552-60.
155. Hiroishi, G., et al., *High D-glucose stimulates the cell cycle from the G1 to the S and M phases, but has no competent effect on the G0 phase, in vascular smooth muscle cells.* Biochem Biophys Res Commun, 1995. **211**(2): p. 619-26.
156. Radhakrishnan, Y., et al., *Insulin-like growth factor-I stimulates Shc-dependent phosphatidylinositol 3-kinase activation via Grb2-associated p85 in vascular smooth muscle cells.* J Biol Chem, 2008. **283**(24): p. 16320-31.
157. Igata, M., et al., *Adenosine monophosphate-activated protein kinase suppresses vascular smooth muscle cell proliferation through the inhibition of cell cycle progression.* Circ Res, 2005. **97**(8): p. 837-44.
158. Wu, W.-y., et al., *Sodium Tanshinone IIA Silate Inhibits High Glucose-Induced Vascular Smooth Muscle Cell Proliferation and Migration through Activation of AMP-Activated Protein Kinase.* PLoS ONE, 2014. **9**(4): p. e94957.
159. Li, H., et al., *Vaspin attenuates high glucose-induced vascular smooth muscle cells proliferation and chemokinesis by inhibiting the MAPK, PI3K/Akt, and NF-kappaB signaling pathways.* Atherosclerosis, 2013. **228**(1): p. 61-8.
160. Park, S.-H., et al., *Neointimal Hyperplasia After Arterial Injury Is Increased in a Rat Model of Non–Insulin-Dependent Diabetes Mellitus.* Circulation, 2001. **104**(7): p. 815-819.
161. Indolfi, C., et al., *Effects of Balloon Injury on Neointimal Hyperplasia in Streptozotocin-Induced Diabetes and in Hyperinsulinemic Nondiabetic Pancreatic Islet–Transplanted Rats.* Circulation, 2001. **103**(24): p. 2980-2986.
162. Wang, K., et al., *Vinpocetine Attenuates Neointimal Hyperplasia in Diabetic Rat Carotid Arteries after Balloon Injury.* PLoS ONE, 2014. **9**(5): p. e96894.
163. Panchatcharam, M., et al., *"Enhanced proliferation and migration of vascular smooth muscle cells in response to vascular injury under hyperglycemic conditions is controlled by β3 integrin signaling".* The international journal of biochemistry & cell biology, 2010. **42**(6): p. 965-974.
164. Mak, K.-H. and D.P. Faxon, *Clinical studies on coronary revascularization in patients with type 2 diabetes*. Vol. 24. 2003. 1087-1103.
165. Frobert, O., et al., *Differences in restenosis rate with different drug-eluting stents in patients with and without diabetes mellitus: a report from the SCAAR (Swedish Angiography and Angioplasty Registry).* J Am Coll Cardiol, 2009. **53**(18): p. 1660-7.
166. Heidari, M., C.A. Mandato, and S. Lehoux, *Vascular smooth muscle cell phenotypic modulation and the extracellular matrix.* Artery Research, (0).
167. Qiu, J., et al., *Biomechanical regulation of vascular smooth muscle cell functions: from in vitro to in vivo understanding.* Journal of the Royal Society Interface, 2014. **11**(90): p. 20130852.

168. Stegemann, J.P., H. Hong, and R.M. Nerem, *Mechanical, biochemical, and extracellular matrix effects on vascular smooth muscle cell phenotype.* J Appl Physiol, 1985. **98**(6): p. 2321-7.
169. Hasaneen, N.A., et al., *Cyclic mechanical strain-induced proliferation and migration of human airway smooth muscle cells: role of EMMPRIN and MMPs.* Faseb J, 2005. **19**(11): p. 1507-9.
170. Hu, Y., et al., *Activation of PDGF receptor α in vascular smooth muscle cells by mechanical stress.* The FASEB Journal, 1998. **12**(12): p. 1135-1142.
171. Williams, B., *Mechanical influences on vascular smooth muscle cell function*: J Hypertens. 1998 Dec;16(12 Pt 2):1921-9.
172. Papadaki, M., S. Eskin, and L.V. McIntire, *Flow modulation of smooth muscle cells (SMC) proliferation and metabolism.* Cardiovascular Pathology, 1996. **5**(5): p. 292.
173. Ueba, H., M. Kawakami, and T. Yaginuma, *Shear stress as an inhibitor of vascular smooth muscle cell proliferation. Role of transforming growth factor-beta 1 and tissue-type plasminogen activator.* Arterioscler Thromb Vasc Biol, 1997. **17**(8): p. 1512-6.
174. Chiu, J.-J., et al., *A model for studying the effect of shear stress on interactions between vascular endothelial cells and smooth muscle cells.* Journal of Biomechanics, 2004. **37**(4): p. 531-539.
175. Koskinas, K.C., et al., *The role of low endothelial shear stress in the conversion of atherosclerotic lesions from stable to unstable plaque.* Current Opinion in Cardiology, 2009. **24**(6): p. 580-590 10.1097/HCO.0b013e328331630b.
176. LaDisa, J.F., Jr., et al., *Alterations in wall shear stress predict sites of neointimal hyperplasia after stent implantation in rabbit iliac arteries.* Am J Physiol Heart Circ Physiol, 2005. **288**(5): p. 14.
177. Papafaklis, M.I., et al., *Relationship of shear stress with in-stent restenosis: bare metal stenting and the effect of brachytherapy.* Int J Cardiol, 2009. **134**(1): p. 25-32.
178. Cifarelli, V., et al., *Human proinsulin C-peptide reduces high glucose-induced proliferation and NF-κB activation in vascular smooth muscle cells.* Atherosclerosis, 2008. **201**(2): p. 248-257.
179. Kobayashi, Y., et al., *Human proinsulin C-peptide prevents proliferation of rat aortic smooth muscle cells cultured in high-glucose conditions.* Diabetologia, 2005. **48**(11): p. 2396-401.
180. Nakamura, J., et al., *Glucose-induced hyperproliferation of cultured rat aortic smooth muscle cells through polyol pathway hyperactivity.* Diabetologia, 2001. **44**(4): p. 480-7.
181. Panchatcharam, M., et al., *Enhanced proliferation and migration of vascular smooth muscle cells in response to vascular injury under hyperglycemic conditions is controlled by beta3 integrin signaling.* Int J Biochem Cell Biol, 2010. **42**(6): p. 965-74.
182. Lin, Y.C., et al., *Resveratrol inhibits glucose-induced migration of vascular smooth muscle cells mediated by focal adhesion kinase.* Mol Nutr Food Res, 2014. **58**(7): p. 1389-401.
183. Chamley-Campbell, J., G.R. Campbell, and R. Ross, *The smooth muscle cell in culture.* Physiol Rev, 1979. **59**(1): p. 1-61.
184. Acampora, K.B., et al., *Development of a novel vascular simulator and injury model to evaluate smooth muscle cell response following balloon angioplasty.* Ann Vasc Surg, 2007. **21**(6): p. 734-41.
185. Kassaian, S.E., et al., *Glycosylated hemoglobin (HbA1c) levels and clinical outcomes in diabetic patients following coronary artery stenting.* Cardiovasc Diabetol, 2012. **11**: p. 82.
186. Marfella, R., et al., *Peri-procedural tight glycemic control during early percutaneous coronary intervention is associated with a lower rate of in-stent restenosis in patients with*

acute ST-elevation myocardial infarction. J Clin Endocrinol Metab, 2012. **97**(8): p. 2862-71.
187. Mazeika, P., et al., *Predictors of angiographic restenosis after coronary intervention in patients with diabetes mellitus.* Am Heart J, 2003. **145**(6): p. 1013-21.
188. Acampora, K.B., et al., *Increased Synthetic Phenotype Behavior of Smooth Muscle Cells in Response to In Vitro Balloon Angioplasty Injury Model.* Annals of Vascular Surgery, 2010. **24**(1): p. 116-126.
189. Chapman, G.B., et al., *Physiological cyclic stretch causes cell cycle arrest in cultured vascular smooth muscle cells.* Am J Physiol Heart Circ Physiol, 2000. **278**(3): p. H748-54.
190. Madi, H.A., et al., *Inherent differences in morphology, proliferation, and migration in saphenous vein smooth muscle cells cultured from nondiabetic and Type 2 diabetic patients.* Am J Physiol Cell Physiol, 2009. **297**(5): p. 9.
191. Faries, P.L., et al., *Human vascular smooth muscle cells of diabetic origin exhibit increased proliferation, adhesion, and migration.* Journal of Vascular Surgery, 2001. **33**(3): p. 601-607.
192. Kumar, A. and V. Lindner, *Remodeling With Neointima Formation in the Mouse Carotid Artery After Cessation of Blood Flow.* Arteriosclerosis, Thrombosis, and Vascular Biology, 1997. **17**(10): p. 2238-2244.
193. Yu, H., et al., *Smooth Muscle Cell Apoptosis Promotes Vessel Remodeling and Repair via Activation of Cell Migration, Proliferation, and Collagen Synthesis.* Arteriosclerosis, Thrombosis, and Vascular Biology, 2011. **31**(11): p. 2402-2409.
194. Perlman, H., et al., *Evidence for the Rapid Onset of Apoptosis in Medial Smooth Muscle Cells After Balloon Injury.* Circulation, 1997. **95**(4): p. 981-987.
195. Qi, Y.X., et al., *Rho-GDP dissociation inhibitor alpha downregulated by low shear stress promotes vascular smooth muscle cell migration and apoptosis: a proteomic analysis.* Cardiovasc Res, 2008. **80**(1): p. 114-22.
196. Shimokawa, H. and A. Takeshita, *Rho-Kinase Is an Important Therapeutic Target in Cardiovascular Medicine.* Arteriosclerosis, Thrombosis, and Vascular Biology, 2005. **25**(9): p. 1767-1775.
197. Li, P.-F., R. Dietz, and R. von Harsdorf, *Reactive oxygen species induce apoptosis of vascular smooth muscle cell.* FEBS Letters, 1997. **404**(2–3): p. 249-252.
198. Han, M., et al., *Smooth muscle 22 alpha maintains the differentiated phenotype of vascular smooth muscle cells by inducing filamentous actin bundling.* Life Sciences, 2009. **84**(13–14): p. 394-401.
199. Hao, H., G. Gabbiani, and M.L. Bochaton-Piallat, *Arterial smooth muscle cell heterogeneity: implications for atherosclerosis and restenosis development.* Arterioscler Thromb Vasc Biol, 2003. **23**(9): p. 1510-20.
200. Pandolfi, A., et al., *Phenotype modulation in cultures of vascular smooth muscle cells from diabetic rats: association with increased nitric oxide synthase expression and superoxide anion generation.* J Cell Physiol, 2003. **196**(2): p. 378-85.
201. Etienne, P., et al., *Phenotype modulation in primary cultures of aortic smooth muscle cells from streptozotocin-diabetic rats.* Differentiation, 1998. **63**(4): p. 225-36.
202. Carrillo-Sepulveda, M.A. and T. Matsumoto, *Phenotypic modulation of mesenteric vascular smooth muscle cells from type 2 diabetic rats is associated with decreased caveolin-1 expression.* Cell Physiol Biochem, 2014. **34**(5): p. 1497-506.